An estimation method for predicting final consolidation settlement of ground improved by floating cement columns

Ishikura, Ryohei; Yasufuku, Noriyuki; Brown, Michael

Published in:
Soils and Foundations

DOI:
10.1016/j.sandf.2016.02.005

Publication date:
2016

AN ESTIMATION METHOD FOR PREDICTING FINAL CONSOLIDATION SETTLEMENT OF GROUND IMPROVED BY FLOATING SOIL CEMENT COLUMNS

Ryohei Ishikura [a]*, Noriyuki Yasufuku [a], Michael J. Brown [b]

[a] *Division of Civil Engineering, Faculty of Engineering , Kyushu University, Japan*

[b] *Division of Civil Engineering, University of Dundee, Dundee, UK*

*Corresponding Author

Abstract

Ground improvement using floating soil cement columns with shallow stabilization is an effective technique for the treatment of deep soft soil layers under infrastructure embankments. In order to investigate the settlement performance of this improvement technique, model load testing of model column analogues for visualization of ground behavior under plane strain conditions was performed and field observations at full scale test embankments were investigated.

The results of model testing and field investigation show that the ground below an embankment founded on a floating column system can be considered as two separate layers with a confined portion and a consolidating layer which can be related to the degree of improvement used at a particular site such as the improvement ratio and the depth of improvement.

A simplified estimation method for final consolidation settlement is proposed using a stress distribution ratio which considers the contribution from skin friction at the surface of floating columns. The advantage of this method is that is possible to determine the consolidating layer thickness as a function of simple parameters such as the degree of improvement, loading conditions and undrained soil strength. The predicted settlements of the improved ground correspond well to that measured in full scale case studies.

Key Words: Ground improvement, Soft soils, Floating soil cement column, Shallow stabilization Consolidation (IGC: E02, K06)

1. Introduction

Reducing cost and environmental impact have recently become important factors influencing the construction and design of soil structures for utilization in key transport infrastructure. Therefore it is essential to develop construction techniques that align with the demands and diversity of current transport infrastructure performance requirements. Ground improvement using cement mixed columns is one effective technique for reducing settlement and stability of deep soft clay deposits under embankments for transport infrastructure such as major highways and rail transport routes. In

this form of improvement, firstly, cement mixed columns are installed (1m diameter is typical in Japan) to a specified depth in soft clay deposits. The upper near surface zone (typically 1-3m in depth) is then excavated and mixed with cement exsitu before replacement and compacted in the excavation to form a shallow stabilized layer.

Where the column tip interacts with underlying competent layers such as dense sand or rock head, the columns are referred to as end bearing columns, which are frequently used, but, shorter floating columns with shallow stabilization are seeing more frequent utilization due to both construction cost savings and reduced raw material use as shown in Fig.1. Furthermore, this combined technology has the potential to be very effective for the treatment of deep soft soil layers where extending columns to a bearing layer is not cost effective or practical to install due to equipment depth limitations.

Based upon the results from full scale monitoring of case studies, the cement mixed floating column (CMFC) technology has been shown to provide acceptable settlement performance for low settlement tolerance road schemes or large infrastructure embankments on soft ground. In order to allow full utilization of this technique, it is essential to develop a simplified design method to predict settlement reduction related to the degree of improvement and insitu soil characteristics such as the improvement ratio, depth of column installation and the soils initial undrained shear strength (Ishikura et al., 2009).

Currently, calculation of the resulting ground settlement with end bearing columns is based upon a

stress distribution ratio approach where the stress is distributed over the soil and columns, and settlement is calculated based upon the ratio of stiffness of the soft clay to the stiffness of the columns, assuming uniform strain below the embankment (Kitazume,2005; Kitazume and Terashi, 2012). This approach has been investigated in detail (Chow et al., 1996; Suksun et al., 2012), but, investigation of the floating type composite ground has received relatively limited attention (e.g., Jung, J.,1999; Ng and Tan, 2014). That said though, methods for predicting settlement of ground improved by floating soil cement columns have previously been proposed (JICE, 1999; Bergado et al., 1994; Miki and Nozu, 2004). Typically these are based on the settlement of two layers, which are considered improved and unimproved as shown in Fig.1. In the method proposed by JICE (1999), an improvement ratio a_p is introduced which is the ratio of the column area to the area of shallow stabilization (or in practical terms the overlying soil structure). If the improvement ratio a_p (%) is more than 30%, the unimproved layer (i.e., that below the columns) is regarded as a consolidating layer; while if a_p (%) is less than 30%, one-third of the improved layer is also regarded as contributing to consolidation settlement. The extent to which the improved layer contributes to settlement (i.e., typically assumed to be one third depth) is thought to have its origins in the concept of the equivalent raft method for calculating pile group settlement (Tomlinson and Woodward, 2008) where the pile group is assumed to transfer the load to the soft soil layer through skin friction at an elevation corresponding to 2/3 of the pile length below the top of the piles.

Determining the extent of the consolidating layer within the improved layer is key to accurate calculation of the system settlement. In order to determine the extent of the consolidating zone within that of the improved layer, a unit cell parametric study using FEM was performed (Chai et al., 2009). From curve fitting of the analytical consolidation settlements, bilinear functions with variables of the improvement ratio and the improvement depth H_1 were proposed to determine the proportion of the consolidating zone within the improved layer. However, this method is still empirical due to the analytical approach and has not been sufficiently validated in relation to the various potential improvement scenarios and other controlling parameters.

Previous work has shown that column skin friction, which is often ignored in settlement assessment, has the potential to be a significant contributor to the behavior of the floating system (Miura et al., 1995,1998). The magnitude of the skin friction contribution has also been shown to be both time and strain level dependent (Ishikura et al., 2013). As the origins of the position of the consolidating layer seems to be linked to the transfer of stress to the surrounding ground via skin friction then the influence of skin friction needs to be fully considered and its effect on the position of the consolidating layer investigated.

Firstly, this study investigates the group effect of the floating column-shallow stabilization composite in a plane strain model soil bed undergoing consolidation with visual observation of settlement. From the results, the influence of improvement variables on the degree of consolidation

settlement and the contribution of skin friction are discussed. By applying image analysis to the model test results, the strain distribution in the improved and unimproved zones was used to inform the likely mechanisms for settlement and the extent of the consolidating zone as well as the degree of contribution from the column skin friction.

Secondly, a simplified method to determine the proportion of the consolidation zone for calculating total settlement of the improved ground is proposed which takes account of improvement conditions (column stiffness, improvement ratio and depth), loading regime and soil strength. The extent of the consolidating zone within the improved layer is obtained based upon a stress distribution ratio which considers the contribution from skin friction at the surface of floating columns. Finally, the validity of the approach is shown through comparisons with field measurements at two different case study sites.

2. Visualization of ground behavior under model plane strain conditions

2.1 Outline of model testing

Fig.2 and Photo1 shows the apparatus used to perform model tests under plane strain conditions. The apparatus consisted of a rigid walled cell of plan area 250 by 100mm and 400mm in depth. The

panels of the container were all made from transparent Perspex which allowed observation of deformation of the model soil on the front face during loading/consolidation. The model arrangement allowed drainage from both the upper plate via a clearance gap of 2.5mm around the outer edge of the upper loading plate and the bottom of the cell via a layer of porous plastic. Wall friction was reduced by placing a rubber membrane between the model soil and the rigid cell wall lubricated with silicon grease.

The model soil consisted of Kaolin clay with properties as summarized in Table 1. The Kaolin clay bed was prepared by forming a slurry with a water content of approximately 80%. The slurry was then carefully poured into the cell up to a depth of approximately 350mm. The cell was initially used to consolidate the soil bed. After that, the clay bed was consolidated under a consolidation pressure σ of 20kPa using an air driven bellofram cylinder until the end of primary consolidation. The latter is determined based on the duration of consolidation relative to the calculated time to the end of primary consolidation (around 500 minutes). After consolidation, a model bed with a height H of approximately 270mm was obtained. This model bed was then extracted from the consolidation cell and wire cut to form the voids required to install the plane strain column analogues (either 1 or 3 were installed), instead of cylindrical column analogues for observing the model ground behavior under the plane strain condition.

The model column analogues were used instead of the actual soil cement columns in order to

homogenize the stiffness and surface roughness of the columns.

The model column analogues were 30mm in width B, 100mm in depth and 200mm in length H_1 and were machined from aluminum (average surface roughness R_a = 0.1-0.3μm). The aluminum columns were then carefully placed in the wire cut slots in the clay and the cell was rebuilt. Vertical loading of the model tests was conducted under stress controlled conditions. The system was designed to allow load to be applied to both the soil bed and the model aluminum column analogue at the same time via the rigid loading plate (simulating the soil-mixed shallow stabilization, Fig.1). Average consolidation pressure σ is calculated by dividing the total load to be applied to both the soil and the model column analogue by the plane area of loading plate. After the model columns were installed, average consolidation pressure σ was re-applied at 20 kPa. During testing, the bed was subject to constant vertical average pressure σ of 40 kPa and 80 kPa which was applied to the bed as quickly as possible using the bellofram cylinder with monitoring until the end of primary consolidation. In addition, the system allowed load to be monitored independently at the head of the columns and the column tips. The monitoring of the column tip loads was achieved via a central shaft running inside the column to a column tip plate. Further detail of this arrangement is described in Ishikura et al., (2012). Loads on the loading plate, column head and column tip were monitored via three independent load cells. Displacement of the top plate which loaded the loading plate was monitored by an electronic dial gauge. During each load increment or consolidation stage, the loads

and plate displacement were monitored at 10 second intervals until the end of primary consolidation.

In order to investigate the deformation behavior of the model soil during consolidation, tracking intersections on the rubber membrane were used. Digital photographs were taken vertically against the front face of the model soil allowing the position and movement of the rubber membranes to be determined at each consolidation stage.

2.2 Test results and discussions

The relationships between the normalized incremental settlement $\Delta S/B$ and the normalized incremental average skin friction $\Delta f/\Delta\sigma$ with elapsed time during the consolidation process with a single column is shown in Fig.3. The incremental average consolidation pressure $\Delta\sigma$ is the difference between the former and current average consolidation pressures. The incremental average skin friction Δf is also calculated by dividing the difference between the incremental load at the head of the column and that at the tip by the side surface area of the model columns (i.e., friction against the perspex ignored due to rubber and lubrication). As shown in Fig.3, the normalized incremental settlement $\Delta S/B$ increased with elapsed time and tended to a constant value. The incremental average skin friction Δf initially increased under application of the incremental average consolidation pressure $\Delta\sigma$. However, after reaching the peak incremental skin friction Δf, the magnitude began to decrease with elapsed time and later converged to a constant value at around 30 minutes after surface

stress application.

The normalized incremental average skin friction $\Delta f/\Delta\sigma$ in $\Delta\sigma$=40kPa became smaller than that in $\Delta\sigma$=20kPa at the constant values. It is thought that one of the reasons for this is the fact that column tip resistance relatively became large due to the soil strength increasing by the soil bed consolidation. Fig.4 shows the relationships between the normalized incremental settlement $\Delta S/B$ and the normalized incremental average skin friction $\Delta f/\Delta\sigma$ under different test conditions. In the 3 columns condition, spacing between centers of column analogue was around 80mm. It is assumed that 2 other columns that do not monitor the loads have the same mobilized frictions during consolidation.

It can be seen from Fig.4 that there are significant differences between the behavior of the single column and that for three columns with far greater skin friction mobilized in the case of the single column throughout consolidation at the lower stress increment. The resulting settlement is also greater for the single column. At the higher stress increment, the normalized incremental mobilized skin friction $\Delta f/\Delta\sigma$ is significantly reduced in magnitude for the single column case and tends to a value similar to that developed by the three column case. Therefore, it is shown that normalized incremental average skin friction $\Delta f/\Delta\sigma$ and normalized incremental settlement $\Delta S/B$ behaviour for a single column is different from that for the 3 columns.

Fig.5 shows images captured of the model soil with a single column before re-applying the consolidation pressure with σ = 0kPa and after the completion of the consolidation process with σ =

80kPa.The deformation vectors were obtained by measuring the differences of node coordinate (nodes at 5mm centres) between the two digital images captured. Based on the deformations measured at the four nodes (or corners) of each element, strain increment calculations and strain contours were determined using strain conversion programs developed in Yamaguchi University, Japan (Yoneda et al., 2013). The degree of deformation induced is clear to the naked eye when comparing Fig 5a and 5b.

Fig.6 shows the deformation behavior of the model soil with a single column and 3 columns after the complete consolidation process where σ has increased from 0kPa (before re-applying) to 80kPa (final average consolidation pressure). Deformation vectors were obtained by observing the soil deformation via the rubber membrane with images recorded before and at the end of the consolidation phase. Vectors are shown magnified by a factor of 3 and 5, respectively (scaling vectors shown above each figure for reference). It was observed that consolidation settlement decreased with an increase of number of columns based upon the magnitude of the vectors.

Considering the single column case, it is shown that there are large vertical soil movements below the loading plate across the complete width of the plate/soil bed. These large vertical displacements continue on moving down the column (increasing depth) but the radial extent reduces rapidly with increasing depth. Towards the base of the column, the radial extent of the displacement is constrained to a limited region close to the column which may be associated with skin friction

resistance. Below the base of the column, there are significant displacements associated with the tip or end bearing resistance. Considering the 3 column case, there is a similar pattern of vertical displacement under the top loading plate but it is clear that the magnitude does not decrease significantly with depth and that there is more consistency in the radial distribution of displacement (i.e., the vertical displacements are relatively uniform throughout the improved layer until the depth tends towards the column tips). Note that the vectors are of different scales for the single and 3 cases and that the relative displacements for the 3 column case are much smaller due to the more even redistribution of stress.

The maximum shear strain distributions for the single column and 3 column cases after consolidation are shown in Fig.7. These strains can be calculated from the deformation behavior in Fig.6. In the single column case, the maximum shear strains are very low below the loading plate down to a depth of approximately $0.25H_1$. The previously highlighted reduction in radial shear strain extent with depth is apparent and there is significant increase in shear strain close to the column which increases with increasing depth and again is significant below the column tip due to the end bearing mechanism. Shear strains in the 3 column case seem to be more evenly distributed with a tendency to increase gradually with depth although significant increases are not noticeable until below the column tips. Definition of any distinct transition in behavior with depth is difficult in either case and more so for the three column case thus suggestions of distinct layer and associated

behavior are tentative..

Fig.8 shows the vertical strains in the soil where the vertical strain is considered to be a result or indicator of consolidation dominant behavior (i.e., where there is zero vertical strain, this is pure downward movement of the soil with the loading plate and columns, and thus consolidation is not occurring). In the single column case, there is a distinct layer below the loading plate where the soil is considered as constrained in that it is moving down with the loading plate and columns thus displaying little vertical strain. At around $0.25H_1$, there appears to be a distinct change in behavior which is consistent with the transition in behavior seen for the shear strain and vertical strains increase with increasing depth suggesting that consolidation is occurring (consolidating improved layer) from $0.25H_1$ down and that above this there is a distinct constrained zone. For the 3 column case the more even distribution of stress results in generally lower vertical strain and it is more difficult to determine the boundary between a distinct constrained zone and a consolidating zone although it appears based upon the level of vertical strain that the proportion of the ground that is likely to be subjected to consolidation would occur at a greater depth and that the constrained zone maybe considered as having a greater depth extent. This suggests that the zone that is consolidating may be lower down the columns in the three columns case with the position being controlled by the magnitude of stress being carried in skin friction which is greater in the single column case. This then gives insights into the thickness of the improved zone that may be considered as undergoing

consolidation.

3. Settlement behavior of full scale of cement column improved ground

Two different full-scale test embankments were constructed on alluvial deposit to investigate the field performance of ground improved by the composite approach of floating soil cement columns coupled to shallow stabilization（Miki et al., 2004; Ishikura et al., 2009）. These dedicated test embankments were constructed close to the development of a section of 55km long carriageway road (National road 208) designed to link the prefectures of Fukuoka, Saga and Kumamoto, around the Ariake sea in the northern part of Kyushu Island, Japan. The test embankments were located close to the town of Shouwabiraki, Fukuoka ,Japan.

The cross sections of the test embankments are shown in Fig.9. The depth of the improved portion was 7.5m in Case 1 and 7.0 to 8.5m in Case 2, due to a variation in the bearing layer elevation. Specific dimensions of the case studies are shown in Fig.9 as the two cases had different thicknesses of shallow stabilization and floating soil cement columns. The case 1 embankment had plan dimensions of 64m by 43.8m and Case 2 was 68.8m by 50.8m. In each case, the improvement ratio was relatively low (Case 1 a_p = 21.7%, Case 2 a_p = 12.0%). The improvement ratio a_p is defined as the ratio of the plan area occupied by the columns to the plan area of the shallow stabilization. Soil

cement columns were constructed by the dry jet cement mixing method, which it was reported that the cement content was around 140 kg/m^3. and were arranged uniformly in a rectangular pattern for Case 1 at approximately 2m centre to centre. In Case 2, the main central area under the embankement had colums spaced at 2.3m centre to centre but as can be seen in Fig.9, this did not extend to the full width of the shallow stabilisation. Therefore, the improvement ratio a_p of Case2 is calculated as the ratio between the plan area of 22m (width of embankment top) by 68.8m and the plan area occupied by the columns in this area. The diameter of the columns was approximately 1.0 m in both cases. The shallow stabilized ground layer was constructed by mixing surface soft clay exsitu with cement and compacted by rolling in layers of controlled thickness to ensure adequate compaction.

In order to examine the consolidation properties of the improved ground, settlement gauges were installed in several layers at known depths at the center of test embankment with the upper gauge placed above the shallow stabilization layer to measure the settlement at the base of the embankment. Fig.10 shows the settlement just below the center of the test embankment after 1 year post embankment construction. In both cases, the soft clay between the columns appears to be confined or constrained in the upper portion of the improved layer and the soil moves down with the settling structure; this suggests that settlement in this zone is associated with the downward movement of the soil rather than due volume change associated with consolidation. Based upon the results of the

previous numerical analysis (Ishikura, 2012), it is suggested that the settlement in the lower part of the improved portion is associated with a gradual increase in consolidation driven volume change. Fig.10 suggests that the improved layer may be considered as two separate layers with an upper confined portion and a a lower consolidating layer.

In order to estimate the final settlement for this improved ground, it is important to determine the thickness of the consolidating layer relative to the degree of improvement represented by the improvement ratio and improvement depth. To simplify the analysis, it is also useful to be able to assume the settling system behaves one dimensionally. This assumption would seem valid based upon observations that the maximum lateral displacements of the embankment toe to the depth were less than 100mm.

4. Estimation method for predicting final settlement

4.1 Homogenized material parameters for representation of composite ground

In order to evaluate the homogenized material parameters for the improved layer using equivalent soil parameters for the soil cement columns and the soft clay, an estimation method for predicting the material parameter for composite ground is used (Omine et al., 1998, 1999). In this figure, H means the depth of soft ground except for the thickness of shallow stabilized ground and H_1 means

the depth of improvement. Fig.11 shows the concept of the homogenized composite ground. In order to evaluate the stress distribution in the composite ground, stress distribution ratio $\bar{n}$ in vertical direction, which is defined as the average of the ratio of the average vertical stress applied to the soil cement column $\overline{\sigma_s}$ and the soft clay $\overline{\sigma^*}$, is introduced in Eq. (1).

$$\bar{n} = \frac{\overline{\sigma_s}}{\overline{\sigma^*}} \tag{1}$$

By using average stress distribution ratio in Eq. (1), the coefficient of volume compressibility of the composite ground in vertical direction is already proposed as follows by Omine et al., (1998).

$$\overline{m_v} = \frac{a_p \bar{n} m_{vs} + (1 - a_p) m_v^*}{(\bar{n} - 1) a_p + 1} \tag{2}$$

Here, a_p is the improvement ratio, and m_{vs} and m_v^* denote the coefficients of volume compressibility of the improved soil cement columns and soft clay, respectively. In order to estimate the value of $\overline{m_v}$, it is important to evaluate the value of $\bar{n}$. This value varies with variation of the degree of improvement.

4.2 Stress distribution ratio estimated based upon skin friction contribution

In order to evaluate the stress distribution ratio $\bar{n}$, it is necessary to determine the magnitude of the skin friction contribution from the floating columns during consolidation. FEM analysis with the original Cam-clay model as the constitutive equation was performed using unit cell axi-symmetric and plane strain models by any variation of the unit cell width and column length (Ishikura et al.,

2006, 2007). Elastic model was also applied to the shallow stabilized ground and columns.

Different series of model soft ground were prepared in both model test and in-situ scales. By applying vertical pre-consolidation pressure or self-weight consolidation, the normally consolidated model soft ground was obtained.

After completing normally consolidated model soft ground with the floating column, the ground surface was deformed evenly based upon the assumption that shallow stabilized ground acted as a rigid plate. In this analysis, compression index C_c (λ = 0.434 C_c) , swelling index C_r (κ = 0.434 C_r) and effective friction angle ϕ ' of model soft ground were 0.60, 0.15 and 31° (M=1.25), respectively. Undrained shear strength ratio which is the ratio of unconfined shear strength to an isotropic pre-consolidation pressure of a normally consolidated model soft ground was introduced in Eq.(3) (Schofield and Wroth, 1968).

$$\frac{c_u}{p_0} = \frac{M}{2}\exp\left(-\frac{\lambda-\kappa}{\lambda}\right) \tag{3}$$

By using this equation, undrained shear strength ratio c_u / p_0 of the numerical model ground was obtained as around 0.295. For simplicity, in this study, in order to assume the undrained shear strength ratio c_u / p_0 of a normally consolidated model soft ground, an initial effective overburden pressure σ'_v was substituted as the value of p_0 which indicates that p_0 is assumed as an isotropic pre-consolidation pressure.

Fig.12 shows the relationship between the resulting skin friction around the surface of the

floating columns and the depth of improvement H_1 normalized by the distance or spacing between columns L after consolidation. In the rectangular pattern improvement condition, spacing between columns is expressed as $L=10r\sqrt{\pi/a_p}$(r is radius of column, a_p is improvement ratio(%)).

An increase in H_1/L means that degree of improvement such as improvement depth and ratio becomes larger. This is shown for a variety of cases including the model testing described above and additional tests on 3D column groups using Kaolin model clay, as reported by Ishikura et al., (2012), as well as numerical modelling of full scale cases. The average skin friction $\bar{\tau}$ is normalized by the initial vertical effective stress which in the case of model tests and numerical modelling of the model test scale is taken as the pre-consolidation pressure and in the numerical modelling of the field case as the pre-installation vertical effective stress at the column base level. The average skin friction is obtained by dividing the difference between the load applied at the head of the floating column and at the tip by the surface area of the floating column after consolidation. Fig.12 shows that the normalized average friction $\bar{\tau}/p_0$ decreases with an increase in H_1/L. This tendency seems consistent for both the model testing and numerical modelling of the full scale in-situ cases.

In this study, the value of $\bar{\tau}/p_0$ can be determined using the proposed formula given in Eq. (4) with the assumption that the maximum value of $\bar{\tau}/p_0$ is less than or equal to the shear strength ratio c_u/p_0.

$$\frac{\bar{\tau}}{p_0} = \frac{c_u}{p_0} \cdot \frac{1}{H_1 / L} \left(\bar{\tau} \leqq c_u\right) \tag{4}$$

Where, the value of around 0.3 were only applied as the undrained shear strength ratio c_u/p_0. It can be seen that the proposed formula in Eq.(4) seems to fit both the model tests and analytical results relatively well. However, this approximated formula in Eq.(4) is expected to work for normally consolidated clays with the undrained shear strength ratio c_u/p_0 of around 0.3. From the soil investigation and sample testing, it was reported that undrained shear strength ratio c_u / p_0 of Alluvial deposits of soft clay around test embankment is also around 0.3. In this paper, Eq.(4) and undrained shear strength ratio of around 0.3 are used for evaluating skin friction contribution from the floating columns.

Any variation in the data points away from the proposed relationship is likely to be influenced by the effect of column surface roughness variations between the analysis and model testing and the magnitude of vertical load applied on the shallow stabilized ground. In the case of FEM, it was assumed that the columns soil interface has the same strength of soft clay. In this paper, average skin friction of column after consolidation is defined assuming that maximum shear resistance of interface between cement mixed column and soft clay is equal to that of soft clay.

In this figure, the approximated formula in the cases of undrained shear strength ratio c_u / p_0 is equal to 0.2 and 0.4 are also shown for reference. Furthermore, it is necessary to confirm the fitting

of Eq.(4) with varying the undrained shear strength ratio c_u / p_0 by performing model testing and numerical analysis under different type of soil conditions.

By using the average skin friction $\bar{\tau}$ in Eq. (4), the average stress distribution ratio after consolidation $\bar{n}$ of the improved portion in Eq. (1) is rewritten in Eq. (5) assuming that the ground surface deforms evenly due to the shallow stabilized ground (Ishikura et al, 2007).

$$\bar{n} = \frac{(D+1)\Delta\bar{\sigma} + \dfrac{\bar{\tau}A_s}{2A_0 a_p}}{\left(\left(\dfrac{D}{R}+1\right)\Delta\bar{\sigma} - \dfrac{\bar{\tau}A_s}{2A_0(1-a_p)}\right)} \tag{5}$$

This equation also has the assumption that the improved soil cement columns and soft clay are independent springs with different stiffness and upward skin friction applied around the surface of the improved soil cement column. These springs deform independently in proportion to the stress applied on them. Where $\Delta\bar{\sigma}$ is the average vertical stress applied over the total improved area, A_0 is the total area of the improved ground, and A_s is the total surface area of columns. D is the depth ratio $H_1/(H–H_1)$, and R indicates the stiffness ratio m_v^* / m_{vs}. By substituting Eq. (5) in Eq. (2), the coefficient of volume compressibility of the improved layer $\overline{m_v}$ is obtained.

4.3 Determination of thickness of improved consolidating layer

Figure 13(a) shows the initial improved ground concept for calculating final settlement in relation to the degree of improvement. When an average vertical stress $\Delta\bar{\sigma}$ is applied to the improved

layer ,it can be considered as having an average coefficient of volume compressibility $\overline{m_v}$ and improvement depth H_1. The compression of the improved layer in the vertical direction is expressed in Eq. (6) as follows:

$$\Delta S_{(a)} = \overline{m_v} H_1 \Delta\overline{\sigma} \quad (6)$$

Unfortunately by this approach and a single $\overline{m_v}$ for the improved layer, it is not possible to distinguish between the influence or the settlement characteristics of the confined portion and the zone of consolidation enclosed within the cement mixed columns and the settling ground below the improved layer, as suggested previously to make this distinction, the improved layer itself is split into two portions where the upper portion is considered as the confined layer and the lower portion as the consolidating layer. This lower portion encompasses both the consolidating improved layer and the consolidating ground below the cement mixed columns (Figure 13(b)). In Figure 13(b), the improvement depth H_1 is now divided into two parts: a confined portion and a consolidating layer within the improved layer. The consolidating layer thickness ratio α in the improved layer is defined as the ratio of the consolidating layer thickness to the total improvement depth H_1. The compression of the improved layer is expressed as follows:

$$\Delta S_{(b)} = \overline{m_{vf}}(1-\alpha) H_1 \Delta\overline{\sigma} + m_v^* \alpha H_1 \Delta\overline{\sigma} \quad (7)$$

Here, $\overline{m_{vf}}$ denotes the coefficient of volume compressibility of the confined portion. The value of

$\overline{m_{vf}}$ is obtained by substituting the stiffness ratio between the column and the soft clay $n_f = m_v^* / m_{vs}$ in Eq. (2). The value of α is expressed in Eq. (8) by assuming that $\Delta S_{(a)}$ is equal to $\Delta S_{(b)}$.

$$\alpha = \frac{\overline{m_v} - \overline{m_{vf}}}{m_v^* - \overline{m_{vf}}} \qquad (8)$$

Table 2 shows the parameters used for calculating the consolidating layer thickness ratio α in the improved layer. α represents the function of general parameters such as degree of improvement, soil properties and loading conditions.

4.4 Characteristics of the consolidating layer thickness ratio

In order to understand the controlling factors that influence the depth of the consolidating layer and thus the magnitude of α, the effects of various parameters on α were investigated. As shown in Table 2, α can be obtained by predicting the $\overline{m_v}$ value of the improved layer. $\overline{m_v}$ is a function of stress distribution ratio $\bar{n}$, improvement ratio a_p, m_{vs} and m_v^* .The stress distribution ratio $\bar{n}$ is influenced by the normalized improvement depth H_1/H, the average skin friction applied on column $\bar{\tau}$ and the average vertical stress on the improved area $\Delta\bar{\sigma}$ in Eq.(5). Furthermore, the average skin friction $\bar{\tau}$ can be determined based upon the undrained shear strength of soft clay c_u in Eq.(4). Therefore 5 parameters including stiffness ratio $R = m_v^* / m_{vs}$, improvement ratio a_p, normalized improvement depth H_1/H, undrained shear strength of soft clay c_u and average vertical

stress on the improved area $\Delta\bar{\sigma}$ are used in this parametric investigation. In order to compare the estimated results with field measurements, the diameter of soil cement column was set at 1 m for parametric investigation.

Fig.14 and 15 show the influence of the stiffness ratio *R* on the factor α which is used to determine the thickness of the consolidating layer. In order to investigate the effect of skin friction magnitude, the values of α are calculated using different undrained shear strengths. The same average vertical stress $\Delta\bar{\sigma}$ which was set at 100 kPa to mimic the design stresses adopted in the previous case studies and normalized improvement depth H_1/H are also applied for calculation. It is clear that the value of α reduces with an increase in improvement ratio and undrained shear strength (i.e., reducing contribution from skin friction). Conversely, the stiffness ratio *R* had little influence on α when R is greater than 50. In this parametric investigation, the stiffness ratio R=100 is applied while investigating influence of the other parameters on α.

Fig.16 shows the influences of improvement ratio and depth on the consolidating layer thickness ratio α_0, where α_0 is the ratio calculated by assuming zero contribution from skin friction. This can be determined by setting the skin friction to zero in Eq.(5) to calculate the appropriate stress distribution ratio and then substituting this in Eq.(2). When skin friction is ignored, the average vertical stress $\Delta\bar{\sigma}$ has no effect on the value of α_0 due to Eq.(5). As shown in this figure, α_0 decreases with an increase of improvement ratio and depth.

Fig.17 shows the effects of soil strength and loading regime on normalized consolidating layer thickness at various degrees of improvement. The relationship between α/α_0 and improvement ratio a_p are constant regardless of normalized improvement depth H_1/H. The values of α/α_0 decrease with an increase of $c_u/\Delta\overline{\sigma}$ and improvement ratio a_p. The consolidating layer thickness ratio α with consideration for the skin friction of a floating column is obtained from α_0 in Fig.16 multiplied by α/α_0 in Fig.17 at the same improvement ratio. As a result, the consolidating thickness layer ratio α in relation to the degree of improvement, soil characteristics and loading conditions can be obtained by using Fig.16 and 17.

4.5 Calculation of settlement of the improved ground

Fig.18 shows the concept for calculating the final settlement of the ground improved by cement mixed columns. In this proposed model, the final settlement is calculated by the summation of one-dimensional consolidation settlements of two layers comprising the confined portion and consolidating layer (i. e., both improved and the lower unimproved zone). Firstly the thickness of the consolidating layer in the improved layer is calculated based upon determination of the value of α which is selected by taking into account the degree of improvement, soil characteristics and the loading conditions. Once the thickness of the consolidating layer in the improved layer has been determined, the compression in the confined zone is calculated from Eq. (9).

$$S_f = \left\{ m_{vs} h_1 + \overline{m_{vf}} (1 - \alpha) H_1 \right\} \Delta\overline{\sigma} \quad (9)$$

Here, m_{vs} and $\overline{m_{vf}}$ denote the coefficient of volume compressibility of the shallow stabilized ground and the confined portion, h_1 is the thickness of the shallow stabilized ground, H_1 is the depth of the improved columns and $\Delta\overline{\sigma}$, the average vertical stress on the improved ground. In the consolidating layer, the average distributed vertical pressure $\Delta\overline{\sigma'}$ is obtained from Eq. (10) under the assumption that average vertical stress $\Delta\overline{\sigma}$ is transferred from the confined portion down to the bottom of consolidating layer evenly as shown in Fig.18.

$$\Delta\overline{\sigma'} = \Delta\overline{\sigma} \times \frac{B}{B'} = \frac{B}{B + \frac{H - (1 - \alpha) H_1}{2}} \quad (10)$$

The settlement of the consolidating layer is obtained by Eq. (11).

$$S_c = m_v^* \left\{ H - (1 - \alpha) H_1 \right\} \Delta\overline{\sigma'} \quad (11)$$

The final settlement of ground improved by floating soil cement columns is calculated by the summation of S_f and S_c as follows:

$$S = S_f + S_c \quad (12)$$

4.6 Design chart for using the two layer α approach

In order to utilize this technique in practice, it is important to select the required degree of improvement to reduce settlement to less than the design acceptable settlement.Fig.19 shows the suggested design procedure flow for utilizing the proposed α approach for settlement calculation.

Soil characteristics and loading conditions are obtained from ground investigation and the design embankment height. An acceptable settlement value is determined to maintain adequate service performance of the embankment.

In order to determine the degree of required improvement such as the improvement ratio and depth, the consolidating thickness layer ratio α is first selected based upon a first estimate of the degree of improvement required, the soil undrained shear strength profile and the loading conditions. Based on this α, final settlement of the improved ground is calculated by Eq.(9), (11) and (12). This process is repeated with varying degrees of improvement until the final calculated settlement *S* is smaller than that of design acceptable settlement.

5. Application of the estimation method to Fukuoka case studies

To confirm the validity of the estimation method for predicting final settlement of the cement mixed column improvement system, estimated final settlement values were compared those measured for case study 1 and 2 shown in Fig.9.As shown in Fig.9, the final embankment heights for both Case 1 and 2 were 8 m. Case 1 had a width of 43.8m and a length of 64m. Case 2 was 50.8m wide with a length of 68.8m. The unit weight of compacted embankment granitic soil was approximately 19.0kN/m^3 in both cases. Site soil characteristics of soft clay obtained from soil

investigation and sample testing are shown in Fig. 20. Alluvial deposits of soft clay extend to approximately 10m depth. The averaged ground water level was 1.0m below ground level. The initial effective overburden pressure σ_v' was calculated by using the wet unit weight of soft clay 16.0 kN/m^3 and the position of the water table.

The average vertical pressure due to the embankment material $\Delta\overline{\sigma}$ was determined by assuming that load from the embankment acted uniformly over the improved area (i.e., the area of the shallow stabilization). The stresses determined $\Delta\overline{\sigma}$ were 102 kPa in Case 1, 109 kPa in Case 2, respectively.

In order to confirm the stiffness ratio of $R = m_v^* / m_{vs}$ for the improved layer, the values of m_v^*, m_{vs} were calculated. The coefficient of volume compressibility of soft clay m_v^* is calculated by Eq.(13).

$$m_v^* = \frac{C_c}{2.3(1+e)p} \tag{13}$$

Here, p is taken as the effective overburden pressure σ_v', prior to embankment installation, at the mid-height of the improved layer $H_1/2$ (Case1 H_1=6.5m, Case2 H_1=5.5m). The void ratio e was taken as 1.8 and compression index C_c was taken as 0.5 and 0.6, respectively, based on the results of the soil investigation. The coefficients of volume compressibility of soft clay were 1.16E-03 m^2/kN in Case1, 9.82E-04 m^2/kN in Case2, respectively. The coefficient of volume compressibility of the column m_{vs} is obtained as the inverse of deformation modulus of E_{50}. E_{50} is also calculated by

using the correlation equation (CDIT, 2002) against unconfined compression strength of the soil cement column q_u, $E_{50}=150q_u$. The average unconfined compression strength of soil cement columns was around 700 (kN/m^2). This results in a stiffness ratio R that is more than 50 which confirms the earlier adoption of R=100.

The undrained shear strength c_u required for determining the consolidating layer thickness ratio α was calculated using initial effective overburden pressure σ_v' under the assumption that shear strength ratio was 0.3. Shear strengths of 16.5 kPa for Case 1 and 18.3 kPa for Case 2, were obtained. On the basis of these parameters and Fig.16 and 17, the consolidating layer thickness ratio α was determined. For the two Cases , the values of α were around 0.33 and 0.49,respectively in spite of the value of C_c (0.5 or 0.6) . The coefficient of volume compressibility of the confined portion $\overline{m_{vf}}$ was obtained by substituting $n_f = m_v^* / m_{vf}$ into Eq.(2). The average coefficient of volume compressibility of the consolidating layer m_v^* was obtained by substituting the compression index C_c and void ratio e into Eq.(13). It is assumed that the average coefficient of volume compressibility of consolidating layer m_v^* is constant with depth. Furthermore, to calculate the average value of m_v^* of the consolidating layer, the geometric mean p in Eq.(14) is substituted into Eq.(13)

$$p = \sqrt{\sigma_v'(\sigma_v' + \Delta\overline{\sigma'})} \qquad (14)$$

Where σ_v' is an initial effective overburden pressure at the mid-height of the consolidating layer in Fig.18, $\Delta\overline{\sigma'}$ is the average distributed vertical stress from the embankment $\Delta\overline{\sigma}$ at the mid-height of

consolidating layer, respectively. Table 3 presents a summary of the parameters determined for calculation of the final settlement.

Fig.21 and 22 show the comparison between the measured settlements and the values calculated for Case 1 and 2 by the proposed and JICE model. The measured values are those measured on the centerlines of the embankments at various depths below the embankments as shown in Fig.9. In the proposed and JICE settlement calculation model, the improved ground was reconsidered as a two layered system that had a uniform coefficient of volume compressibility. Therefore, the settlements of the improved ground change linearly in several layers. As shown in this figure, consolidating layer thickness in relation to the degree of improvement by this proposed model became larger than that of JICE model in both Cases regardless of compression index C_c . The calculated settlement values correspond well to the measured settlements by this proposed model incorporating the effect of the position of the improved consolidating layer.

Fig.23 and 24 show the comparison of calculated settlements by this proposed and JICE model with improvement ratio a_p in Case1 and 2.

As shown in these figures, the discontinuity of the calculated values by JICE model can be seen at around 30% of improvement ratio a_p. On the other hand, the calculated settlement can be expressed in continuous numerical values with an increase in improvement ratio a_p by this proposed model regardless of compression index C_c.

6. Conclusions

This study has proposed an estimation method for final consolidation settlement of composite cement mixed floating columns and shallow stabilization below transport infrastructure embankment construction based upon the findings model loading tests enhanced with soil deformation visualization techniques and field measurements at full scale study sites with up to 10 m of soft soil deposits. The following conclusions are obtained:

(1) Settlement behaviour of a model composite stabilization regime during consolidation was investigated by load testing under plane strain condition. In the single column case, it was observed based upon vertical strain magnitude that there was an apparent boundary between a discreet constrained zone (where soil was deformed vertically) and consolidating zone (within the length of the column analogue). In addition, it was also identified that the constrained zone increased in depth with an increase in the number of columns through comparison with a 3 column case.

(2) The findings from laboratory investigation were consistent with field observation at full scale embankment construction trials. Field settlement measurements below the full scale embankment

also suggested that the improved layer can be divided into two separate layers with a confined portion and a consolidating layer where their thicknesses could be related to the degree of improvement at each site.

(3) Through comparison of the results of this study and previous FEM analysis, average skin friction around the surface of the floating columns after consolidation was shown to decrease with increasing degree of improvement represented by the improvement ratio and depth. This tendency seems to be consistent for both the model testing and numerical modelling and can be represented by an empirically derived formula as a function of shear strength ratio and degree of improvement.

However, in the near future, in order to get the more general results, it is necessary to investigate the influence of the undrained shear strength and over consolidation ratio on the skin friction after consolidation.

(4) A simplified estimation method for predicting final consolidation settlement of the floating soil cement column composite stabilization technique below an embankment has been proposed which uses a simple stress distribution ratio based on the magnitude of the shear stress at the column soil interface. The advantage of this method is that it allows determination of the consolidating layer thickness as a function of simply derived parameters such as the degree of improvement, loading

conditions and undrained soil strength**.**

(5) The calculated settlement values for the of the floating soil cement column composite stabilization technique below an embankment correspond well to the full scale measured settlements with incorporating the effect of the position of the improved consolidating layer and the influence of shear stress at the column-soil interface on the position of this layer..

Acknowledgments

The first author wishes to express his gratitude to the many students at the graduate school of Yamaguchi University, for their experimental support. The first author is also grateful to Prof. Yukio Nakata of Yamaguchi University for his support in image analysis. the authors would like to acknowledge the helpful advice and encouragement provided by Professor Hiroshi Matsuda of Yamaguchi University and Professor Kiyoshi Omine of Nagasaki University .

References

Bergado, D.T., Chai, J.C., Alfaro, M.C., Balasubramaniam, A.S., 1994. Improvement Techniques of Soft Ground in Subsiding and Lowland Environment, *Taylor and Francis*,pp.108 –121.

Chai, J.-C., Miura, N., Kirekawa, T., Hino, T., 2010. Settlement prediction for soft ground improved by columns. Ground Improvement, Proceedings of Institute of Civil Engineering, UK, Vol. 163, No. 2, pp. 109-119.

Chow, Y.K., 1996. Settlement Analysis of Sand Compaction Pile, Soils and Foundations, Soils and Foundations,36(1), 111-113.

Coastal Development Institute of Technology(CDIT), 2002. The Deep mixing Method, Principle, Design and Construction, Balkema, pp.42-44.

Ishikura, R., Matsuda, H., Igawa, N., 2013. Visualization of Settlement Behavior for Friction Pile Group during Consolidation, *Proceedings of 18th International Conference on Soil Mechanics and Geotechnical Engineering*, pp.2759-2762.

Ishikura, R., Matsuda, H., Yasufuku, N., Omine, K., Kashima, K., Igawa, N., 2012. Settlement behavior of piled raft foundation in soft ground, *Proceedings of the 9th International Conference of on Testing and Design Methods for Deep Foundation*, pp.485 -490.

Ishikura, R., 2012. Settlement control of the improved ground by combination of surface stabilization and floating type cement-treated columns, Proceedings of 7th Asian Young Geotechnical Engineer Conference, Tokushima, Japan, pp.289-296.

Ishikura, R., Ochiai, H., Omine, K., Yasufuku, N., Matsuda, H. and Matsui, H., 2009. Evaluation of the settlement of in-situ improved ground using shallow stabilization and floating-type cement-treated columns, Journal of JSCE(C):65(3),745-755(in Japanese).

Ishikura, R., Ochiai, H., Matsui, H., 2009. Estimation of settlement of in-situ improved ground using shallow stabilization and floating-type columns, *Proceedings of 17th International Conference on Soil Mechanics and Geotechnical Engineering*, pp.2394-2398.

Ishikura, R., Ochiai, H., Omine, K., Yasufuku, N.,T., Kobayashi., 2007. Estimation of the settlement of improved ground with a combined technology of shallow stabilization and floating-type cement treated columns, *Journal of Geotechnical Engineering.*, JSCE , 63(4), pp.1101–1112 (in Japanese).

Ishikura, R., Ochiai, H., Yasufuku, N., Omine, K., 2006. Estimation of the settlement of improved ground with floating-type cement-treated columns, *Proceedings of the 4th International Conference*

on Soft Soil Engineering, Vancouver, Canada, pp. 628–635.

Japanese Institute of Construction Engineering (JICE), 1999. Flexible foundation , Foundation structure part. In Design Code for Flexible Box Culvert- II (Chapter4), San-kai-dou Press, Tokyo, pp.233-248(in Japanese).

Jung, J., Moriwaki, T., Sumioka, N., Kusakabe, O., 1999. The consolidation behavior of clay ground improved by partly penetrated SCP, Journal of Geotechnical Engineering, JSCE,III-46,617,101-113(in Japanese).

Kitazume, M., Terashi, M., 2012. The deep mixing method, CRC Press, *Taylor and Francis*, pp.296-pp305.

Kitazume, M., 2005. The Sand Compaction Pile Method, CRC Press, pp.12.

Ng, K.S., Tan, S.A., 2014. Design and analyses of floating stone columns, Soils and Foundations,54(3), 478-487.

Miki, H., Nozu, M., 2004. Design and Numerical Analysis of Road Embankment with Low Improvement Ratio Deep Mixing Method, Geotechnical Engineering for Transportation Projects, ASCE, pp. 1395-1402.

Miki, H., Inoue, Y., Okochi, Y., 2004. Comparison between observed data of full-scale test embankments on soft clay and 3D analysis, 4th seminar on soft ground improvement in high way construction. , pp.77–85.

Miura, N., Wen-Jing WU, Nakamura, R., Ichinose, T., 1995. Experimental Study on Skin Resistance of Pile in Soft Clay,Journal of Geotechnical Engineering, JSCE, III-31, 517, 63-72 (in Japanese).

Miura, N., Shen, S., Koga, K., Koga, K., Nakamura, R., 1998. Strength Change of Clay in the Vicinity of Soil-Cement Column, JSCE, III-43, 596, 209-221(in Japanese)

Omine, K., Ochiai, H., Yoshida, N., 1998. Estimation of in-situ strength of cement-treated soils based on a two-phase mixture model, Soils and Foundations, 38(2), 17-29.

Omine, K., Ochiai, H., Bolton, M.D., 1999. Homogenization method for numerical analysis of

improved ground with cement- treated soil columns, Dry Mix Methods for Deep Soil Stabilization, Balkema, pp.161-168.

Schofield, A. N. and Wroth, C.P., 1968. Critical state soil mechanics, McGraw-Hill, London, 161-165.

Horpibulsuk, S., Chinkulkijniwat, A., Cholphatsorn, A., Suebsuk, J.,Liu,M.D., 2012. Consolidation behavior of soil-cement column improved ground, Computers and Geotechnics, 43, 37-50.

Tomlinson,M.J., Woodward, J., 2008. Pile design and construction practice, *5th Edition,Taylor and Francis*,pp.240-243.

Yoneda, J., Hyodo, M., Yoshimoto, N., Nakata, Y., Kato, A., 2013. Development of high-pressure low-temperature plane strain testing apparatus for methane hydrate-bearing sand, Soils and Foundations 53(5), 774-783.

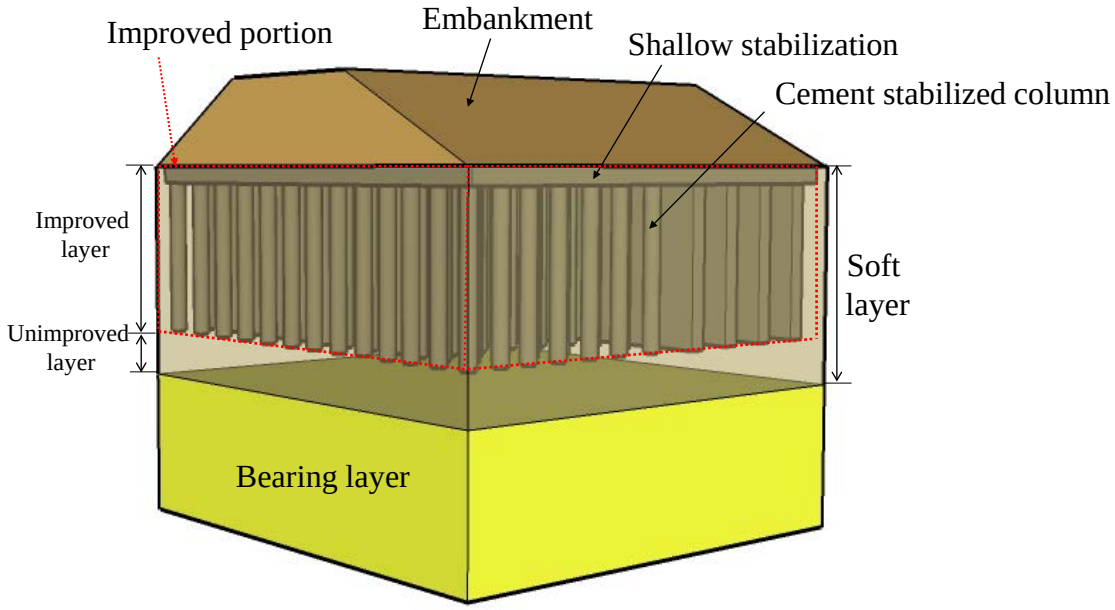

Fig.1 Schematic representation of shallow stabilization by the floating cement mixed column method.

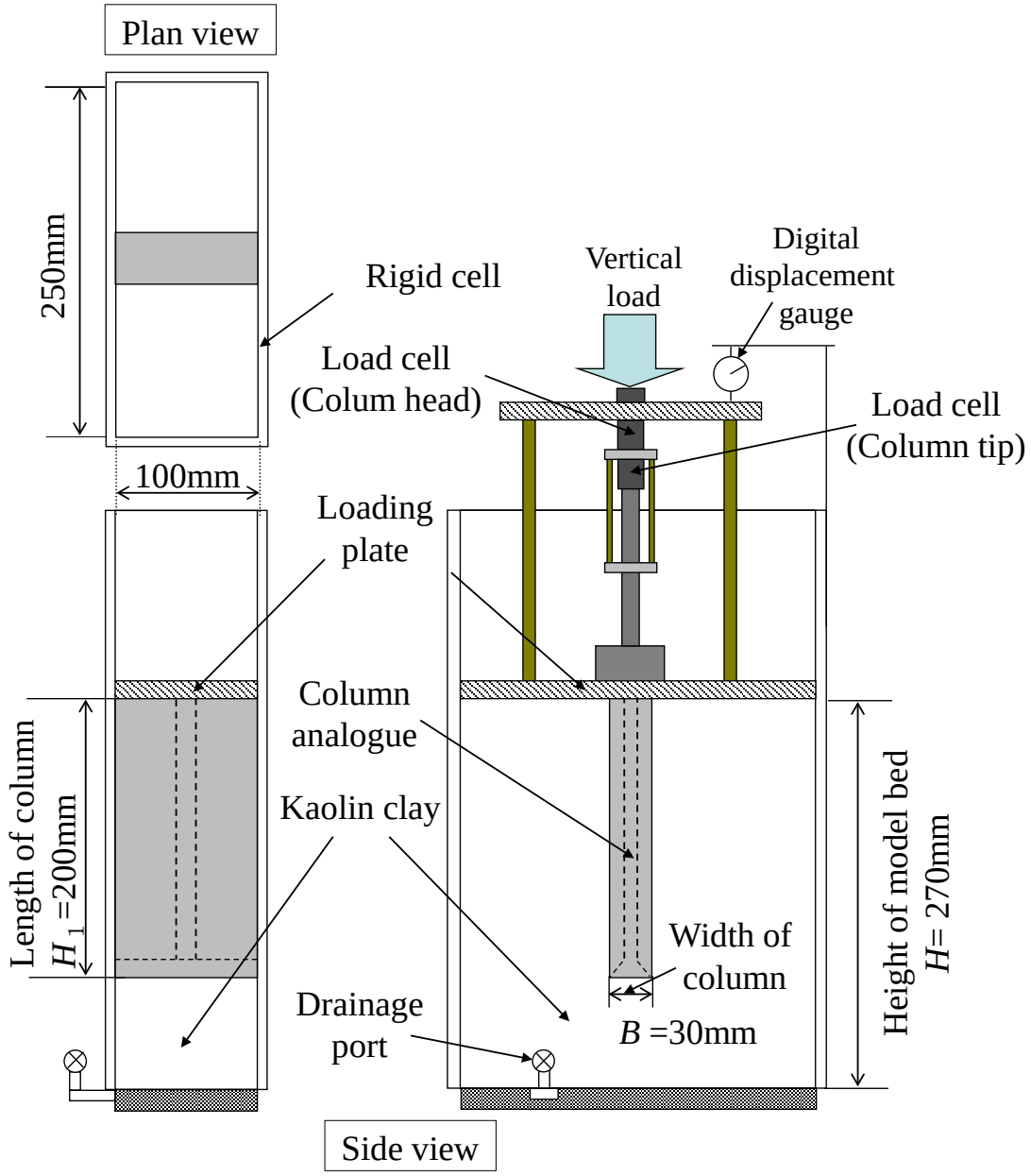

Fig.2. Schematic of the plane strain model testing arrangements

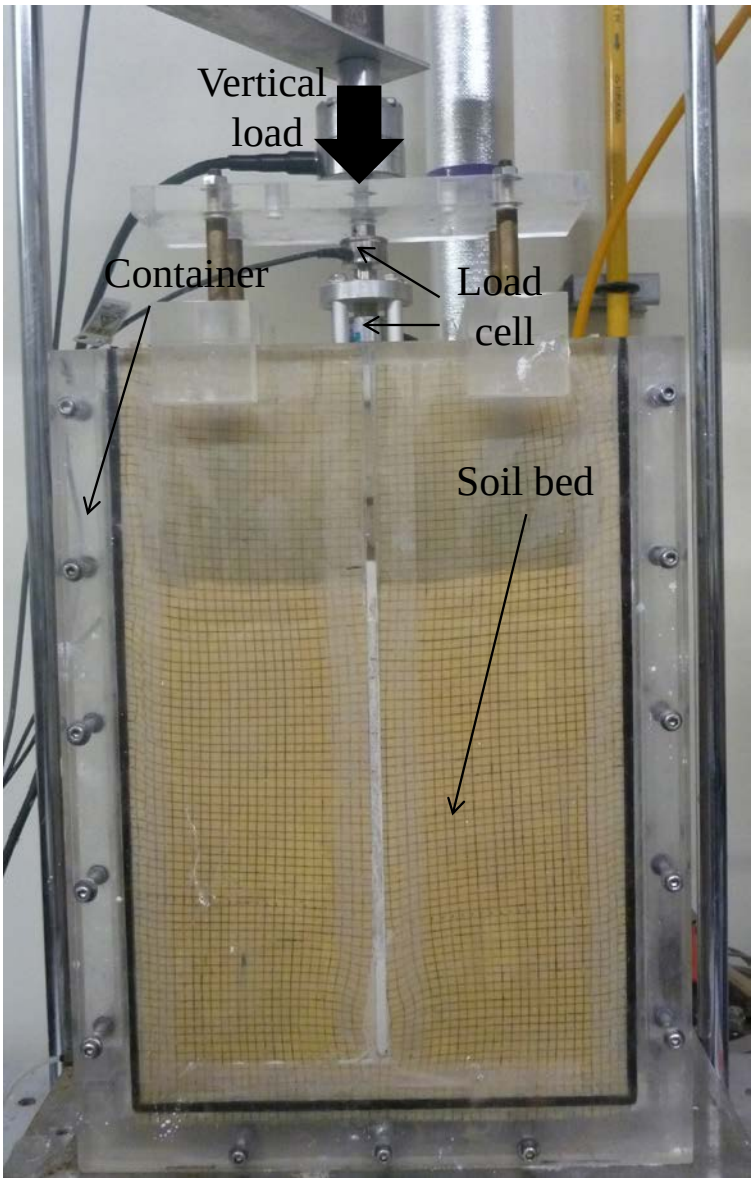

Photo1 Plane strain model testing apparatus.

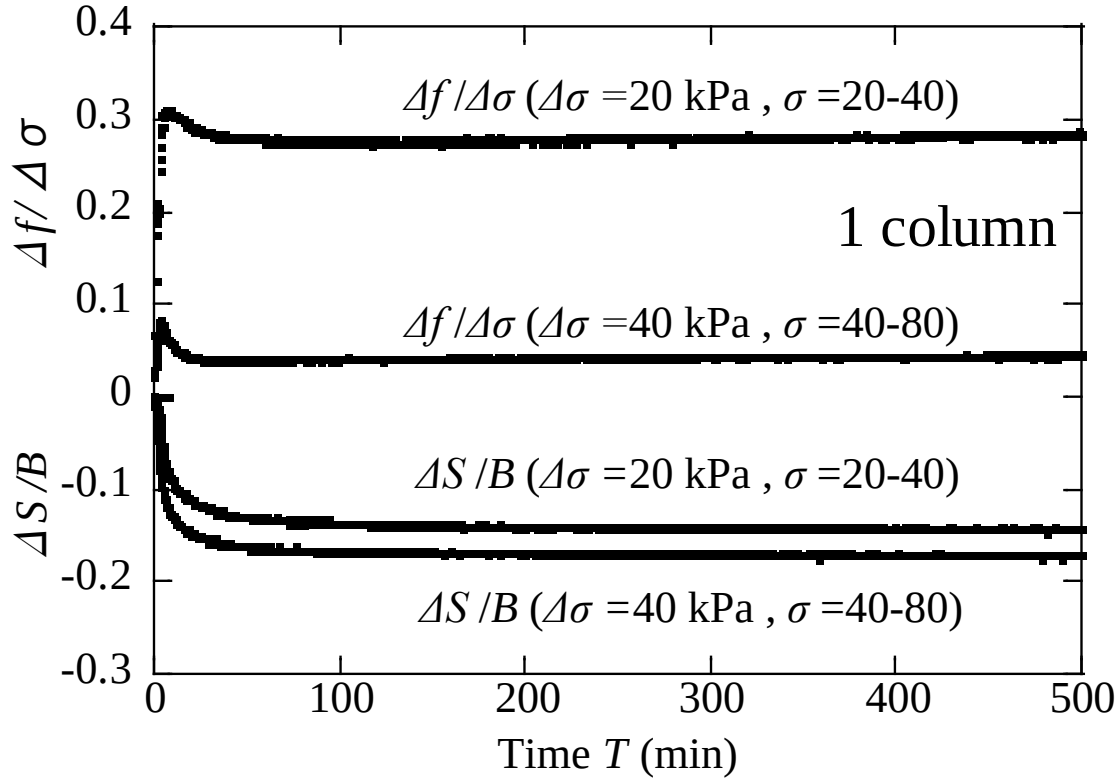

Fig.3. Relationship between skin friction, consolidation settlement and elapsed time for the single column case.

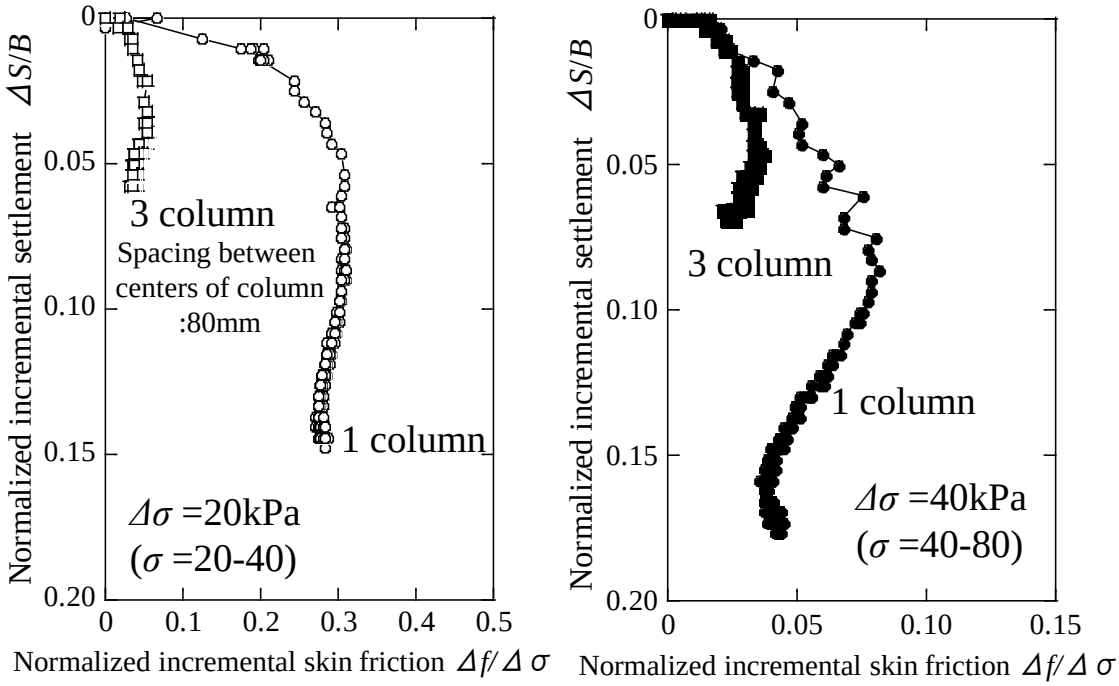

Fig.4. Comparison of the normalized settlement and skin friction for the 1 column and 3 column cases.

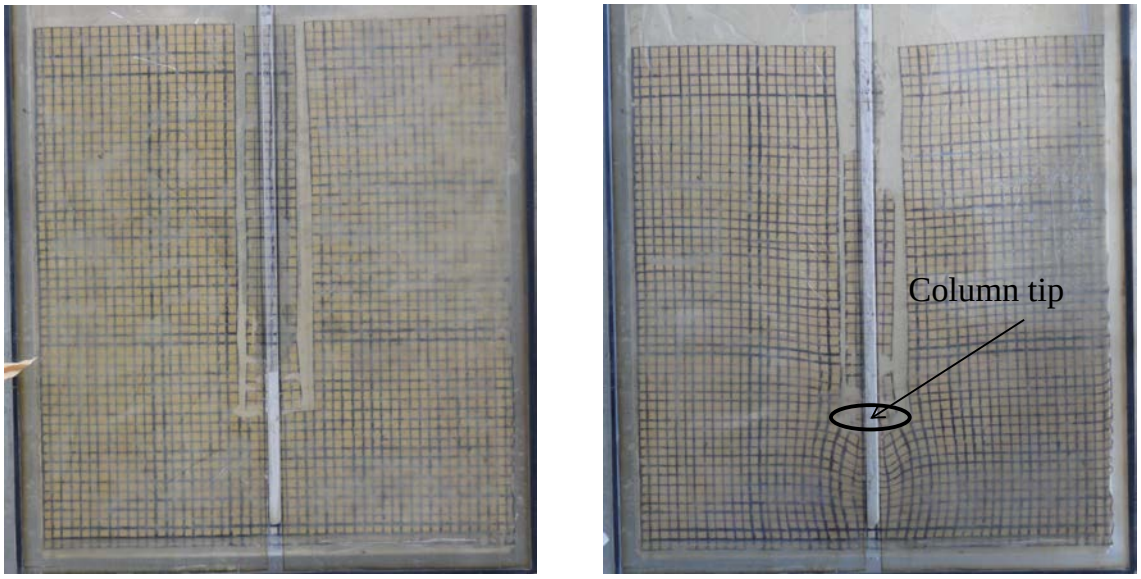

Fig.5. Images captured before and after consolidation in the single column case;

a) Before re-applying the consolidation pressure (σ = 0kPa),

b) After the complete consolidation process where (σ =80kPa).

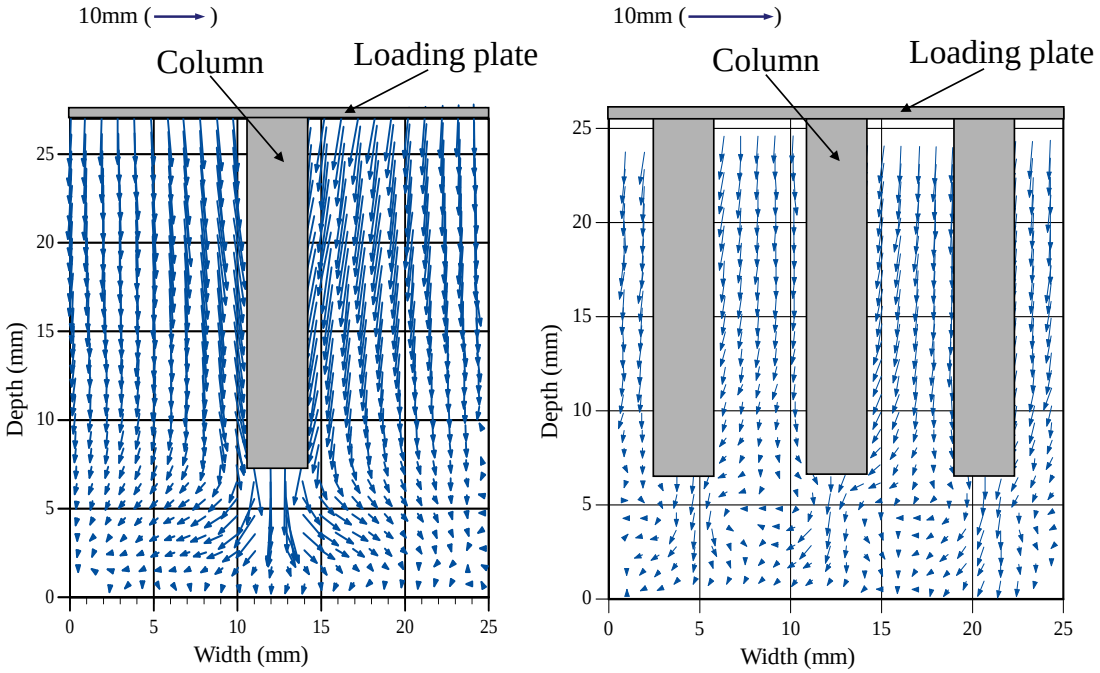

Fig.6. Deformation vectors in the model soil, a) Single column case (vectors scaled up ×3), b) 3 column case (vectors scaled up ×5), Note scaling vector shown above each figure .

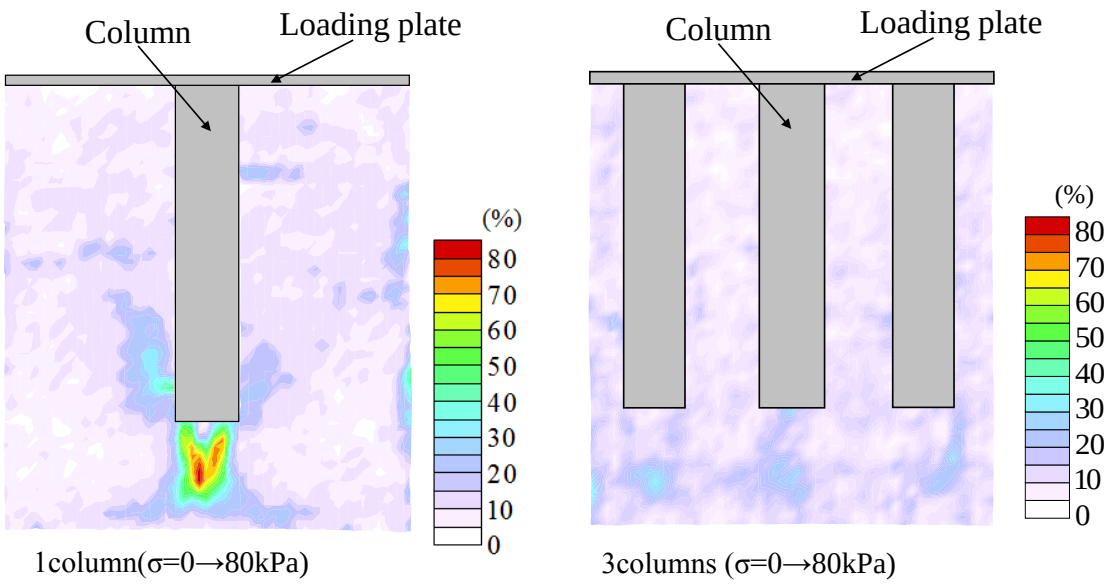

Fig.7. Comparison of the maximum shear strain distribution as a result of the consolidation process.

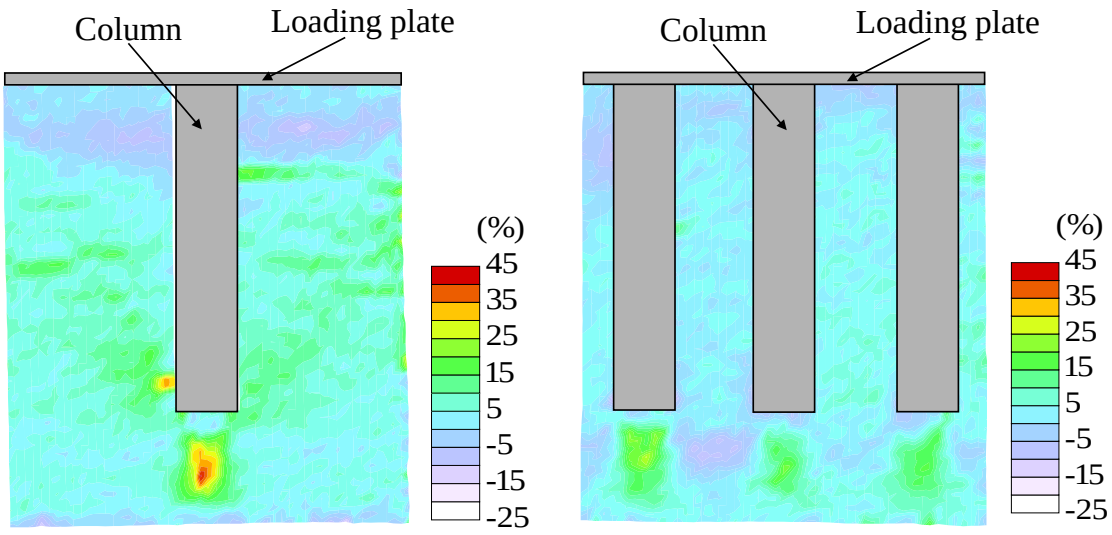

Fig.8. Comparison of the vertical strain distributions as a result of the consolidation process.

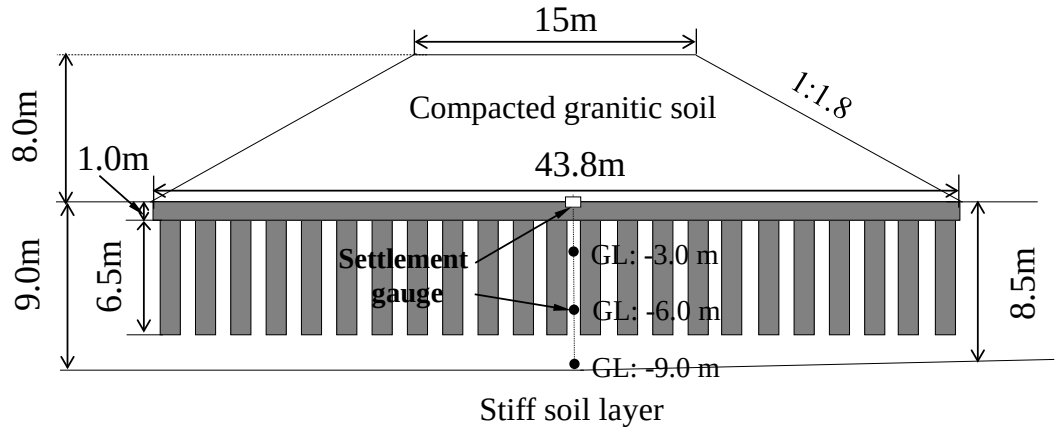

Case 1: Improvement ratio: a_p=21.7%

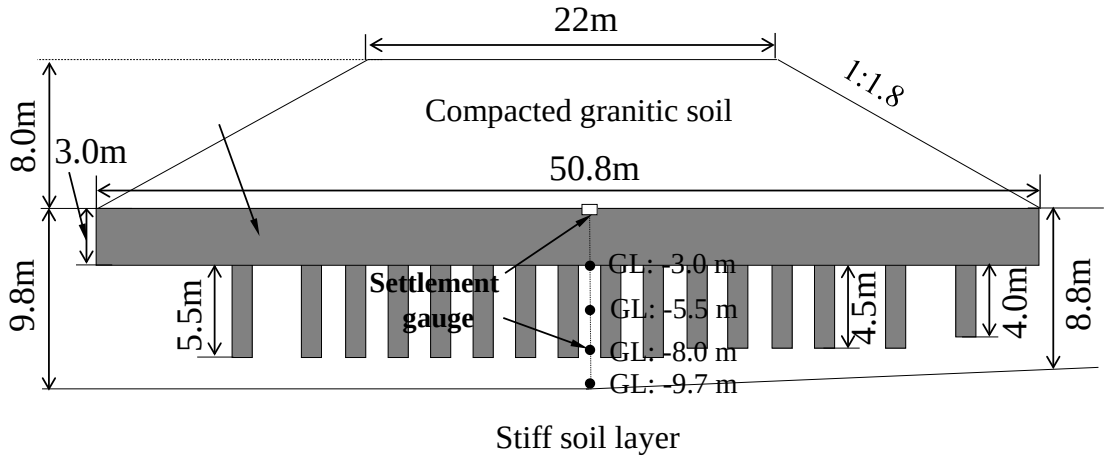

Case 2: Improvement ratio: a_p=12.0%

Fig.9. Cross-section through the two case study full scale test embankments.

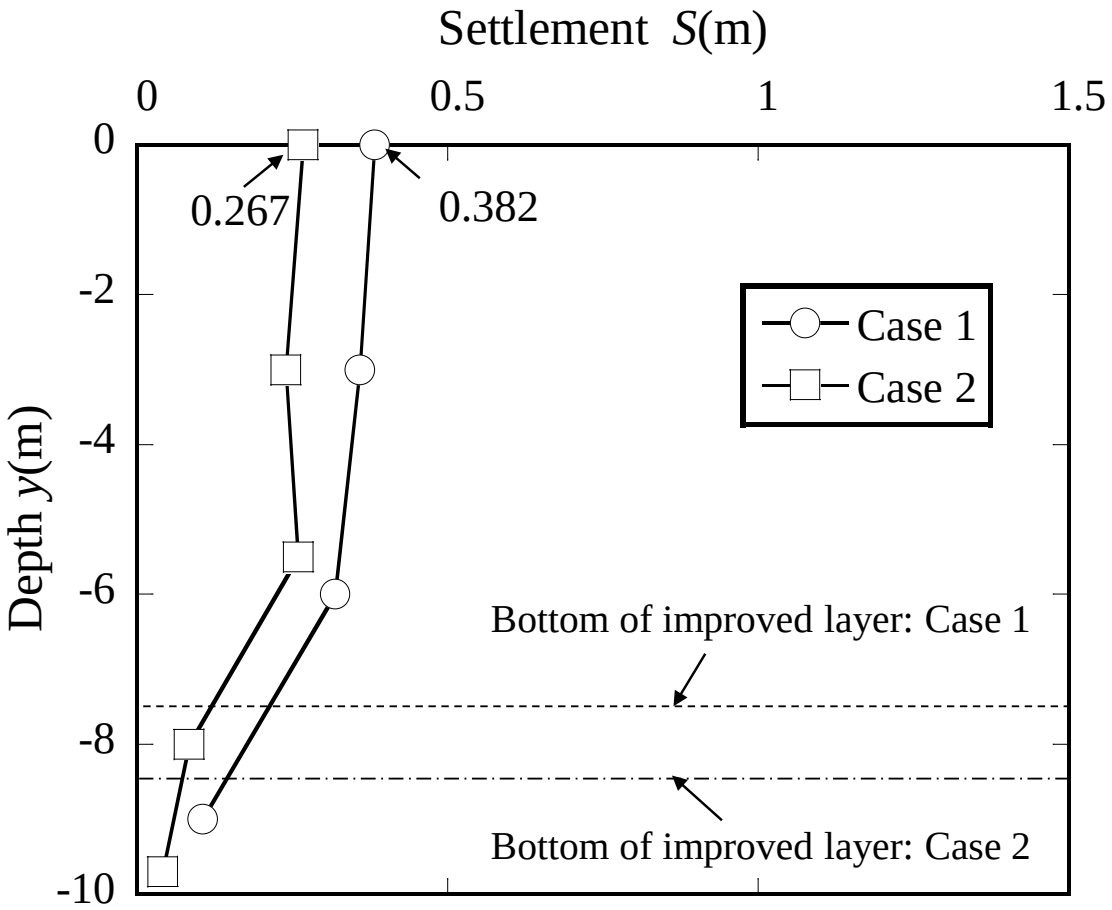

Fig.10. Measured settlements below the center line of the test embankments.

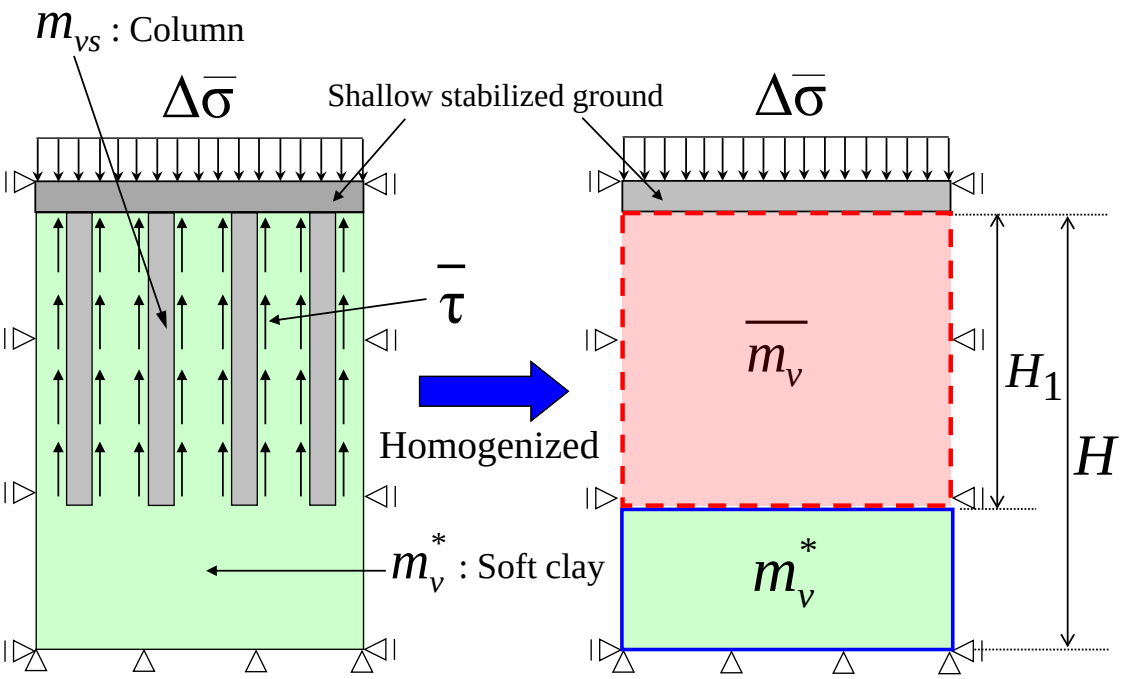

Fig.11. Schematic representation of the homogenized composite ground with floating cement mixed columns.

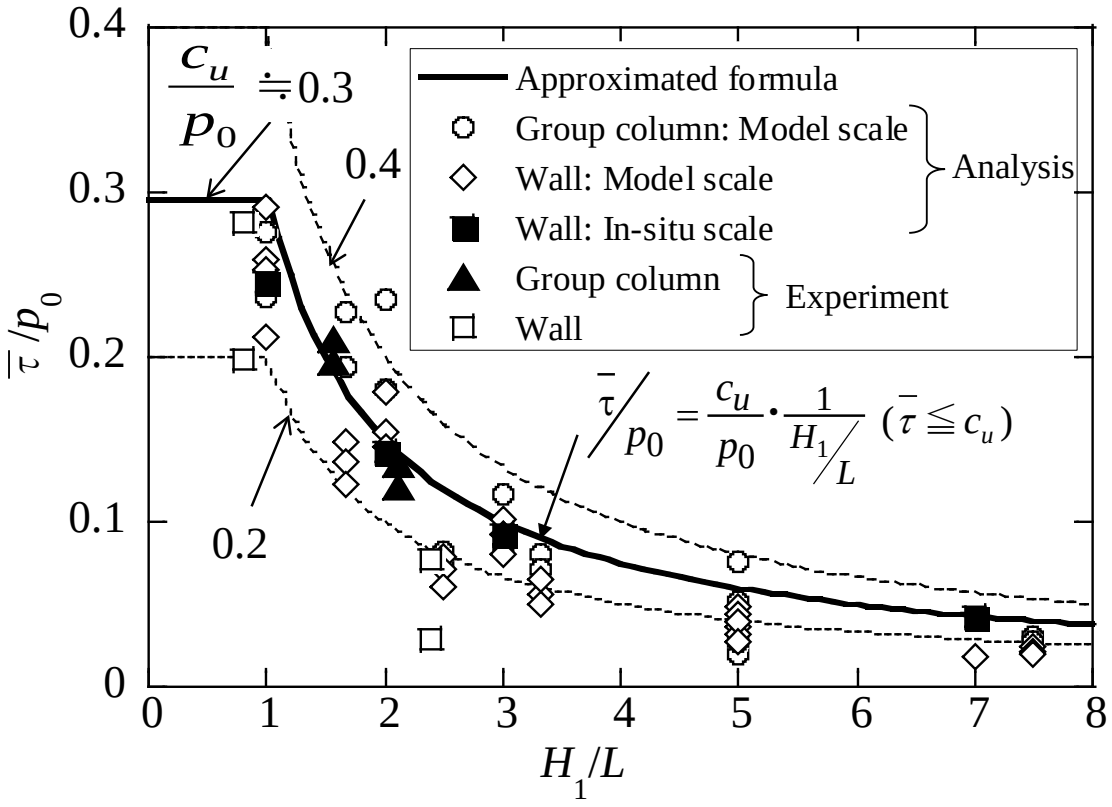

Fig.12. Variation of normalized average skin friction with degree of improvement.

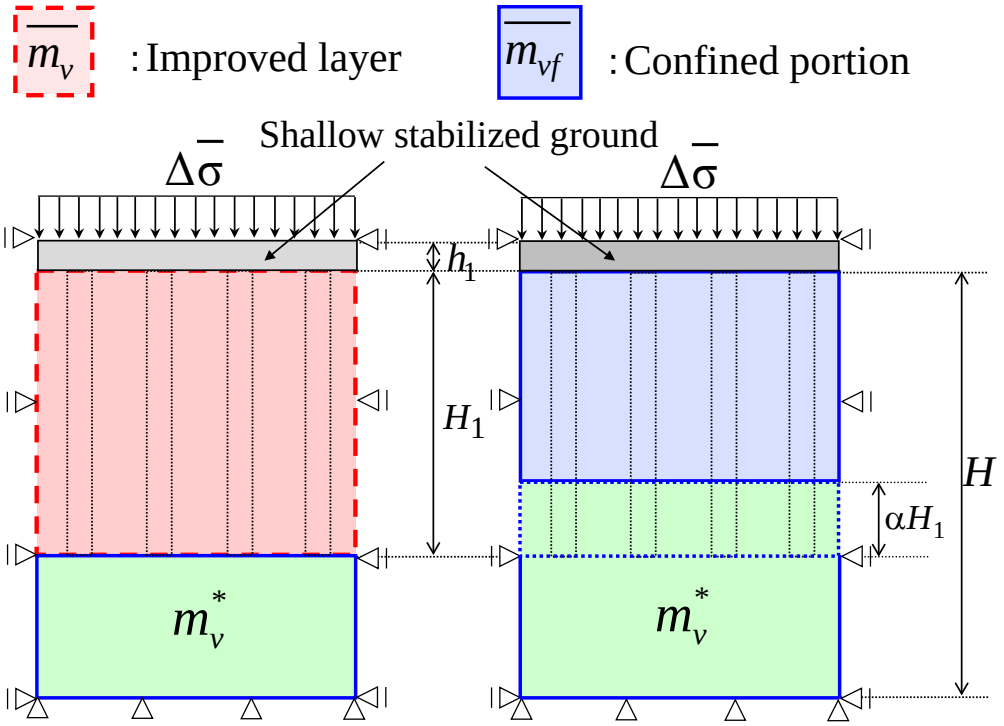

(a) Initial improved ground concept (b) Two layer improved ground concept

Fig.13. Schematic showing the conceptual approaches to layer and stiffness determination.

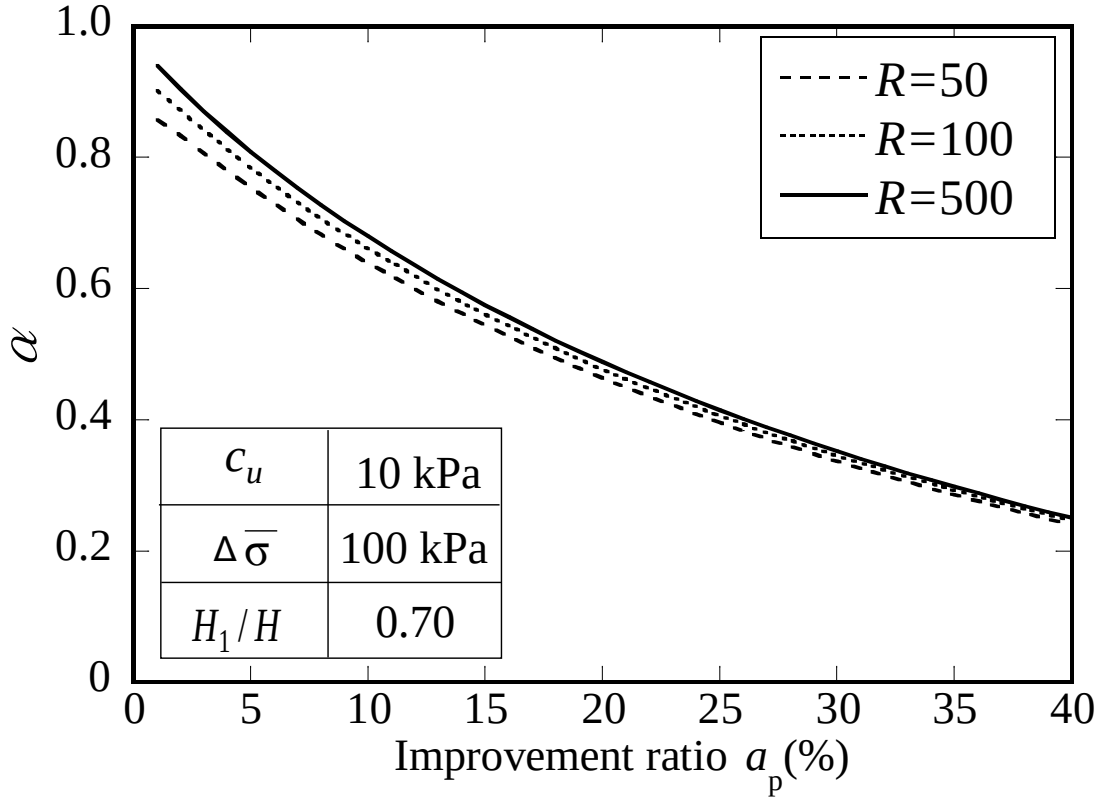

Fig.14. Influence of the stiffness ratio *R* on the consolidating layer thickness ratio(α) (c_u=10kPa).

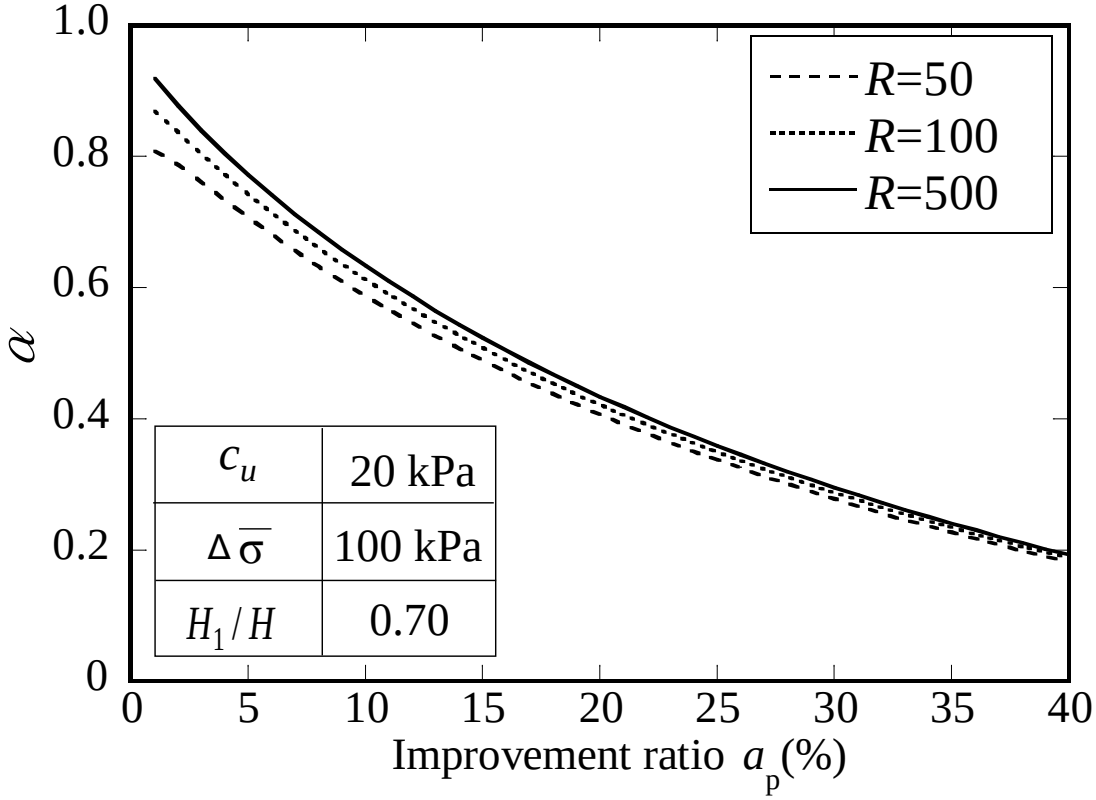

Fig.15. Influence of the stiffness ratio *R* on the consolidating layer thickness ratio(α) (c_u=20kPa).

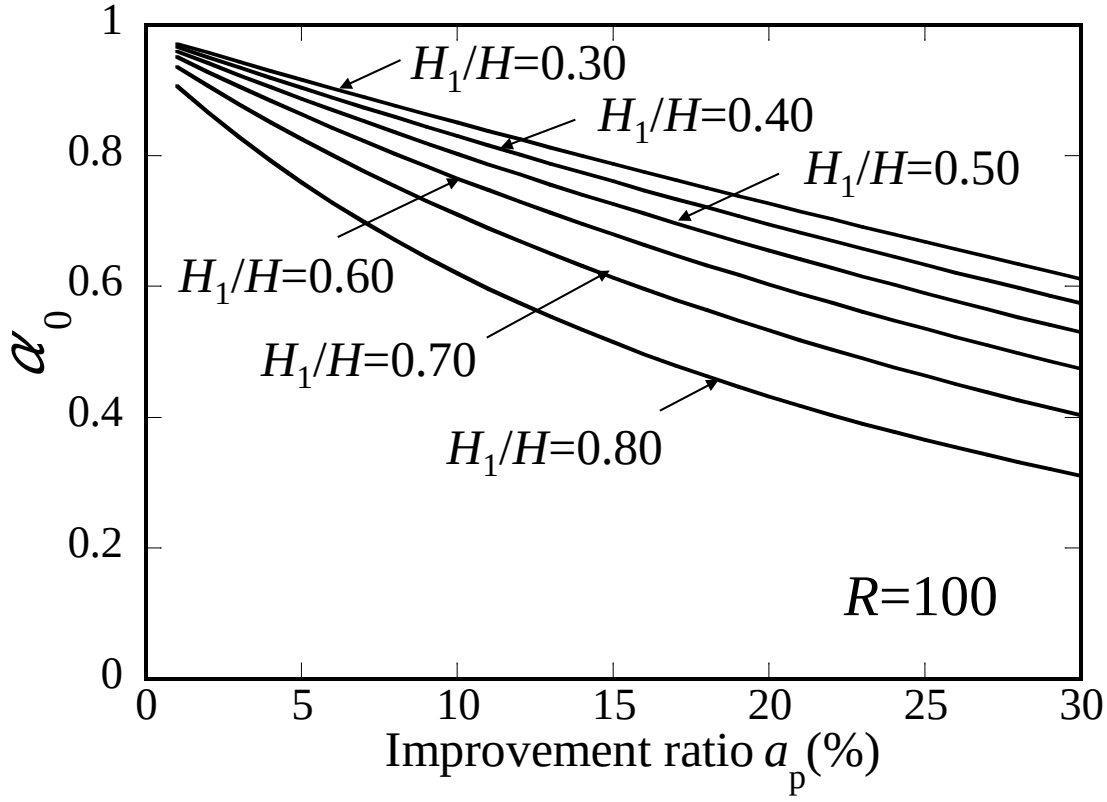

Fig.16. Effect of degree of improvement on the α_0 (R=100) .

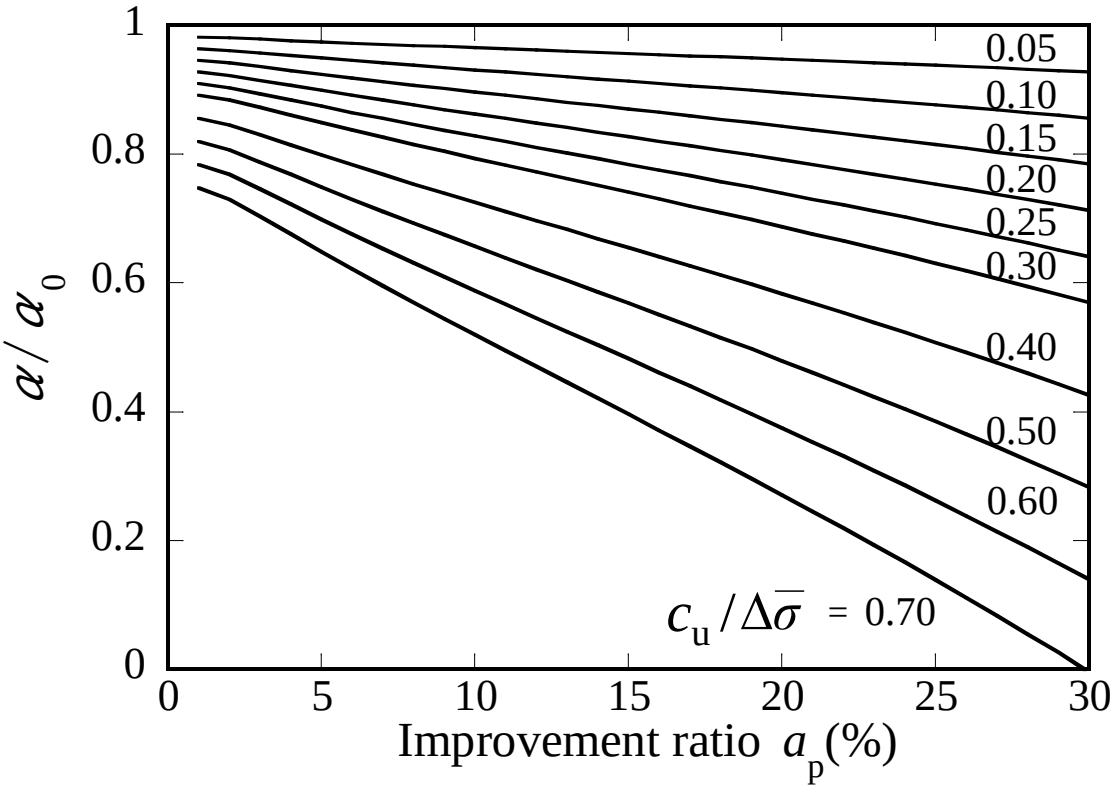

Fig.17. Effect of soil characteristic and loading conditions on the normalized consolidation depth ratio.

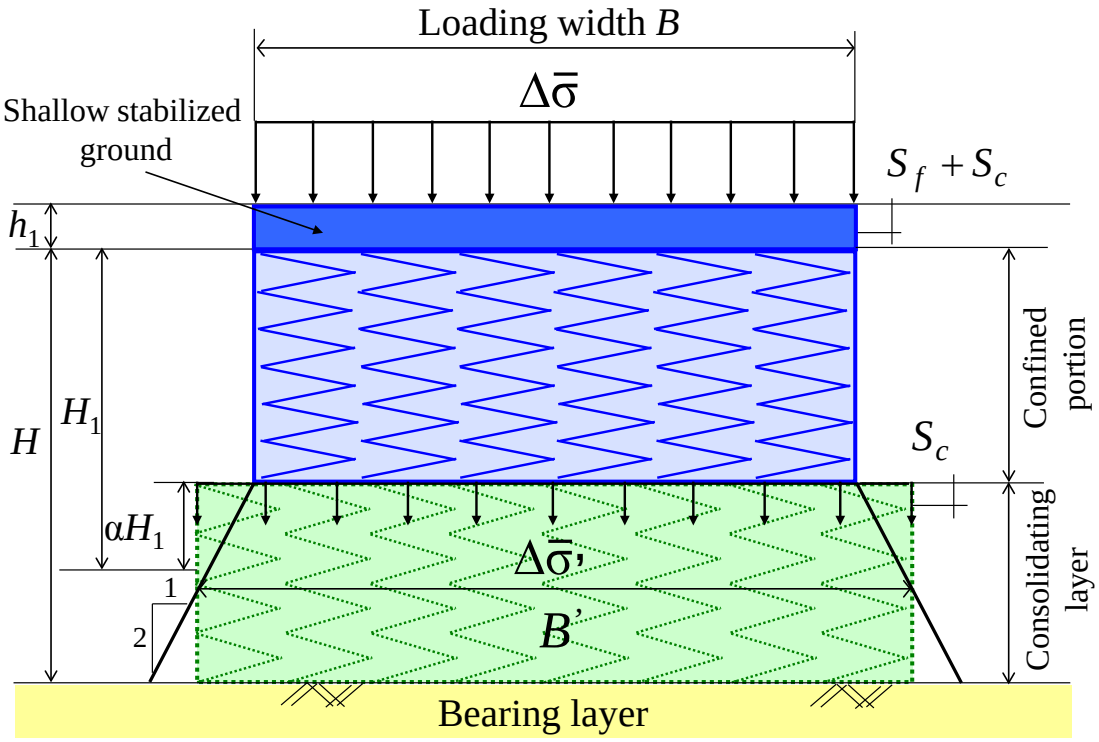

Fig.18. Schematic showing the concept for calculating the final settlement of the improved ground.

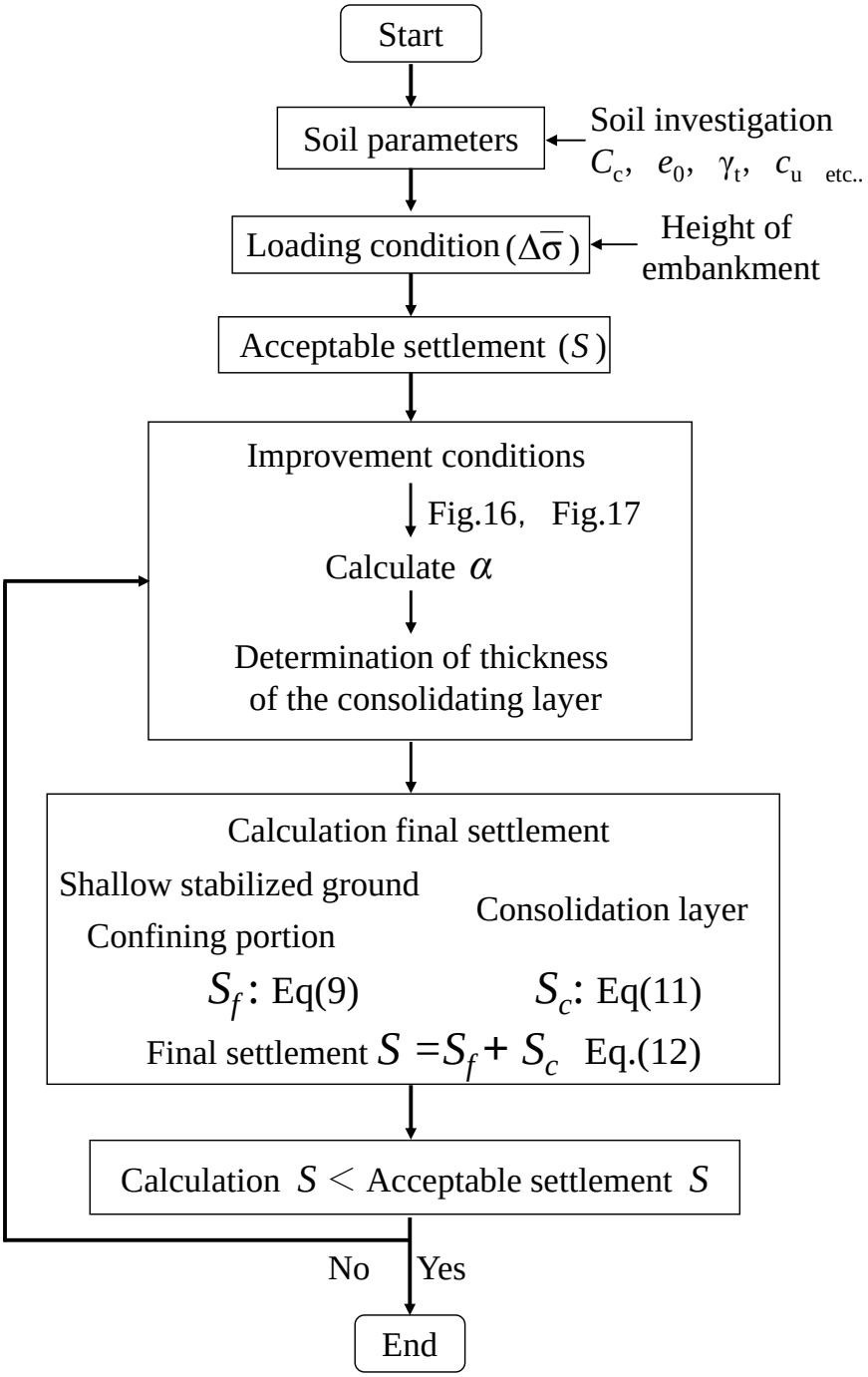

Fig.19. Design flow chart for determing the degree of improvement required to meet design settlement limits.

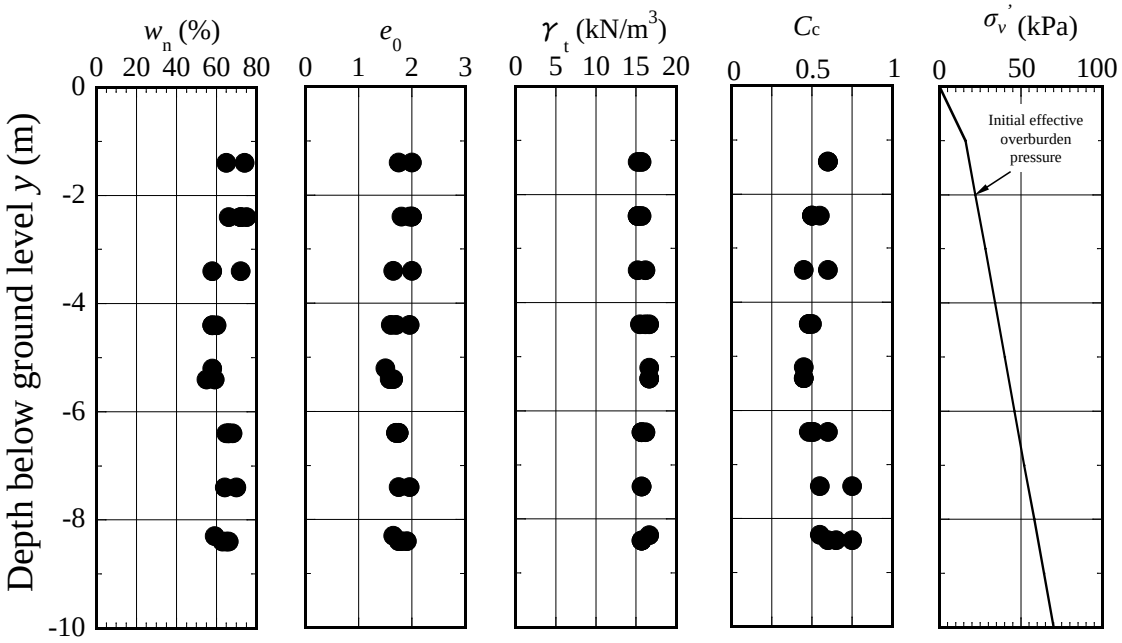

Fig.20. Soil characteristics determined for the ground under test embankments.

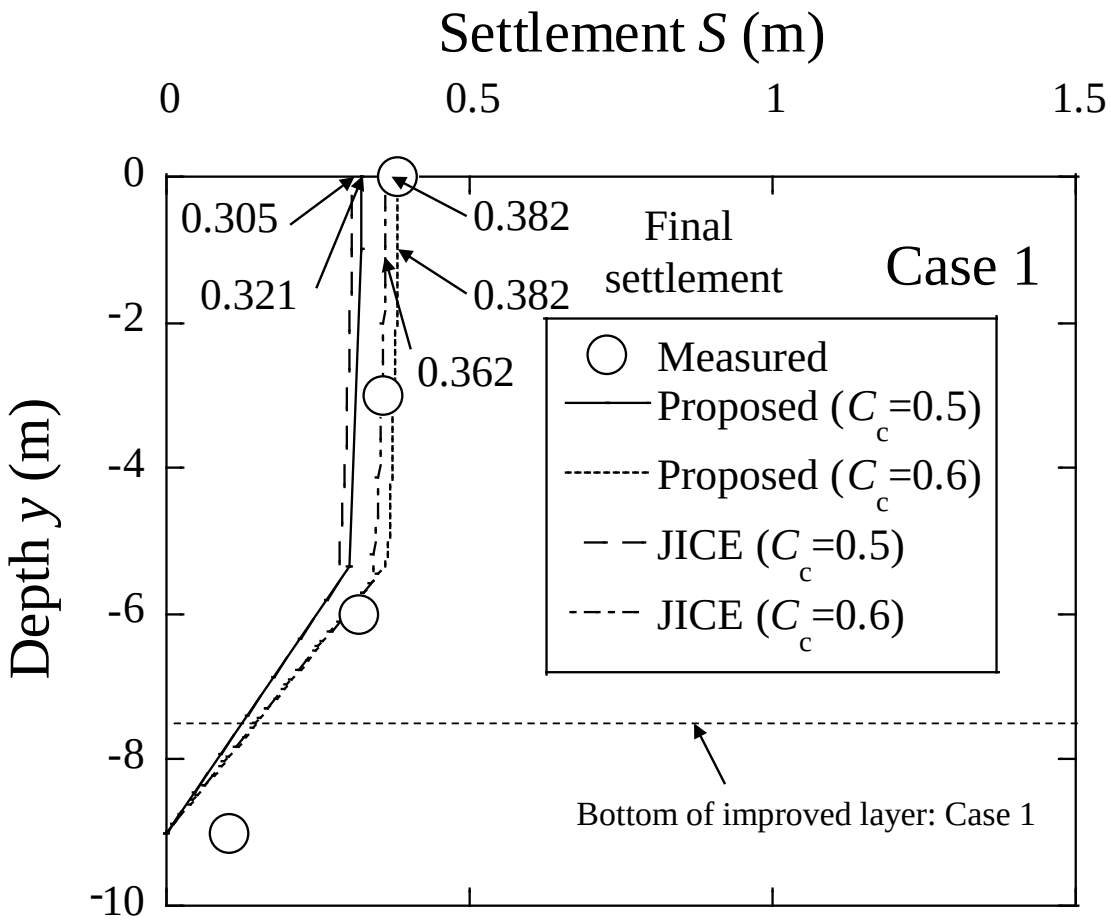

Fig.21. Comparison of calculated settlement values with those measured below the embankment (Case1).

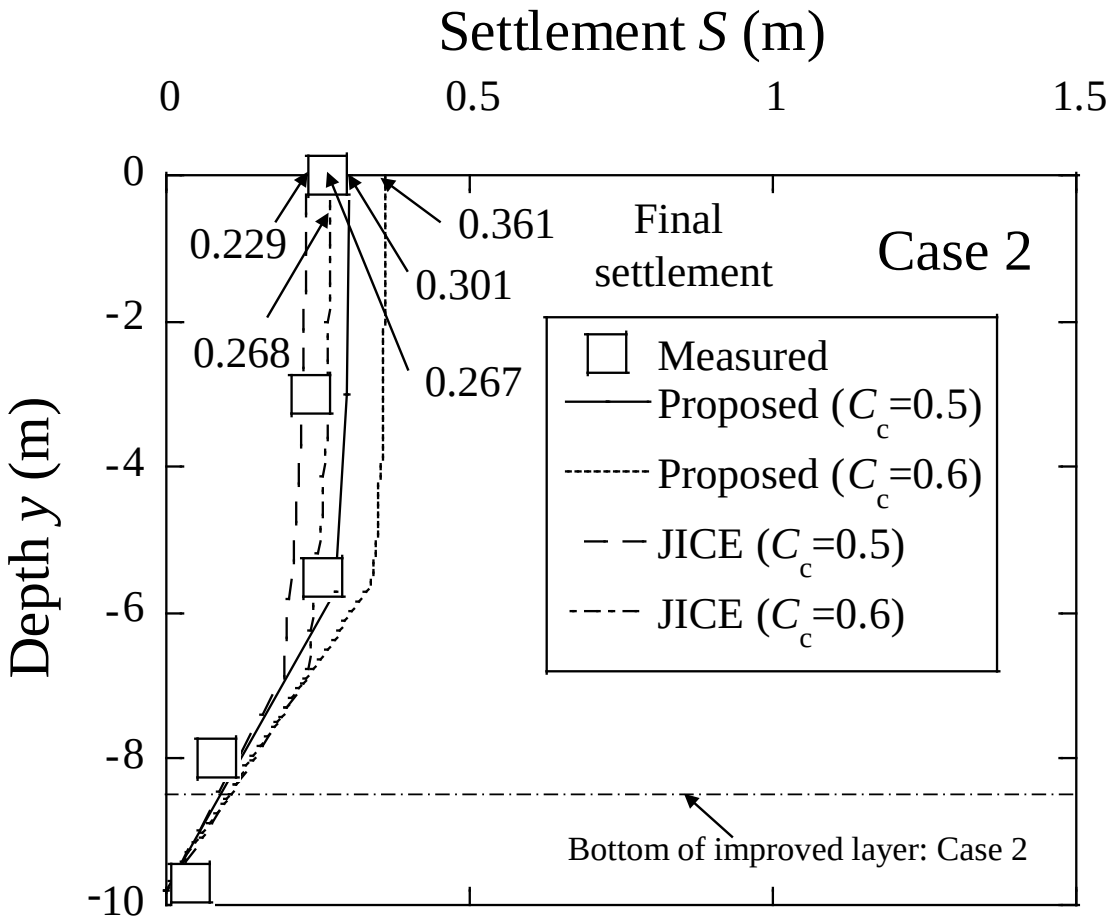

Fig.22. Comparison of calculated settlement values with those measured below the embankment (Case2).

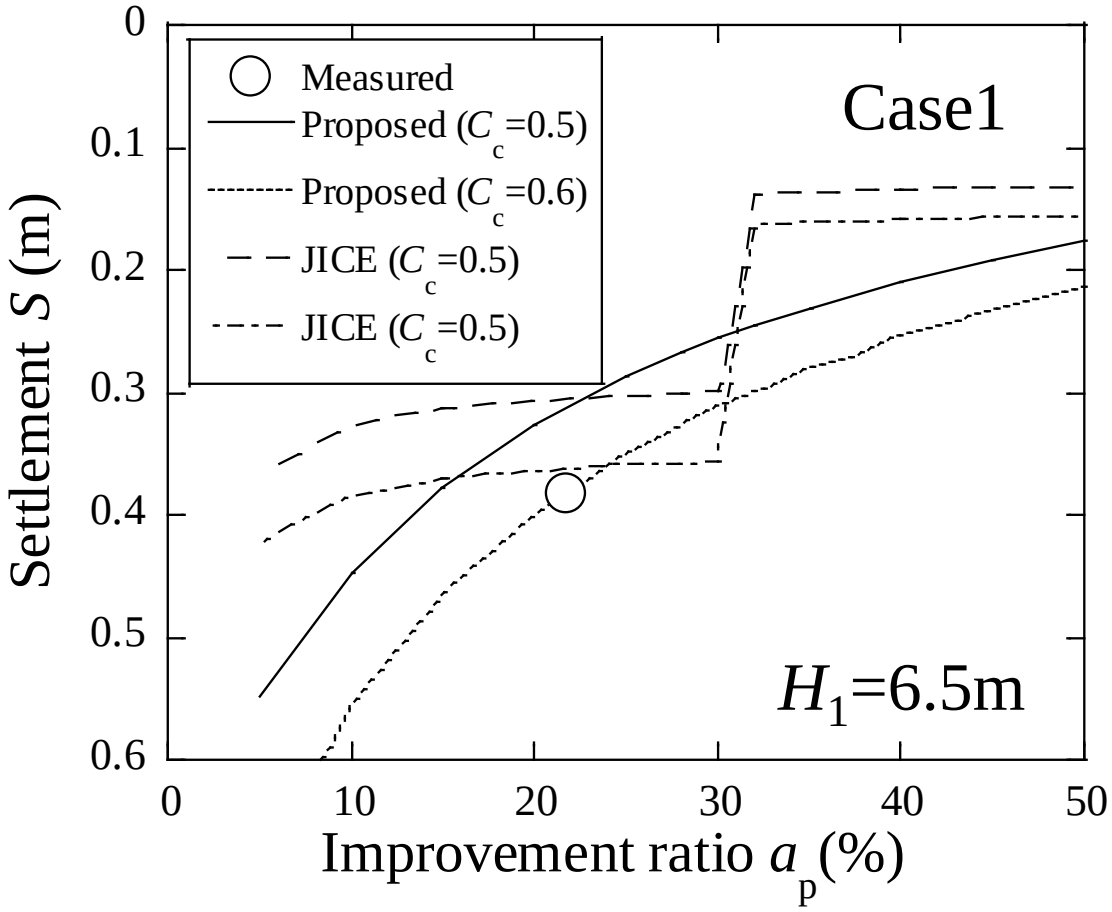

Fig.23.Comparison of calculated settlements by this proposed and JICE model with improvement ratio (Case 1).

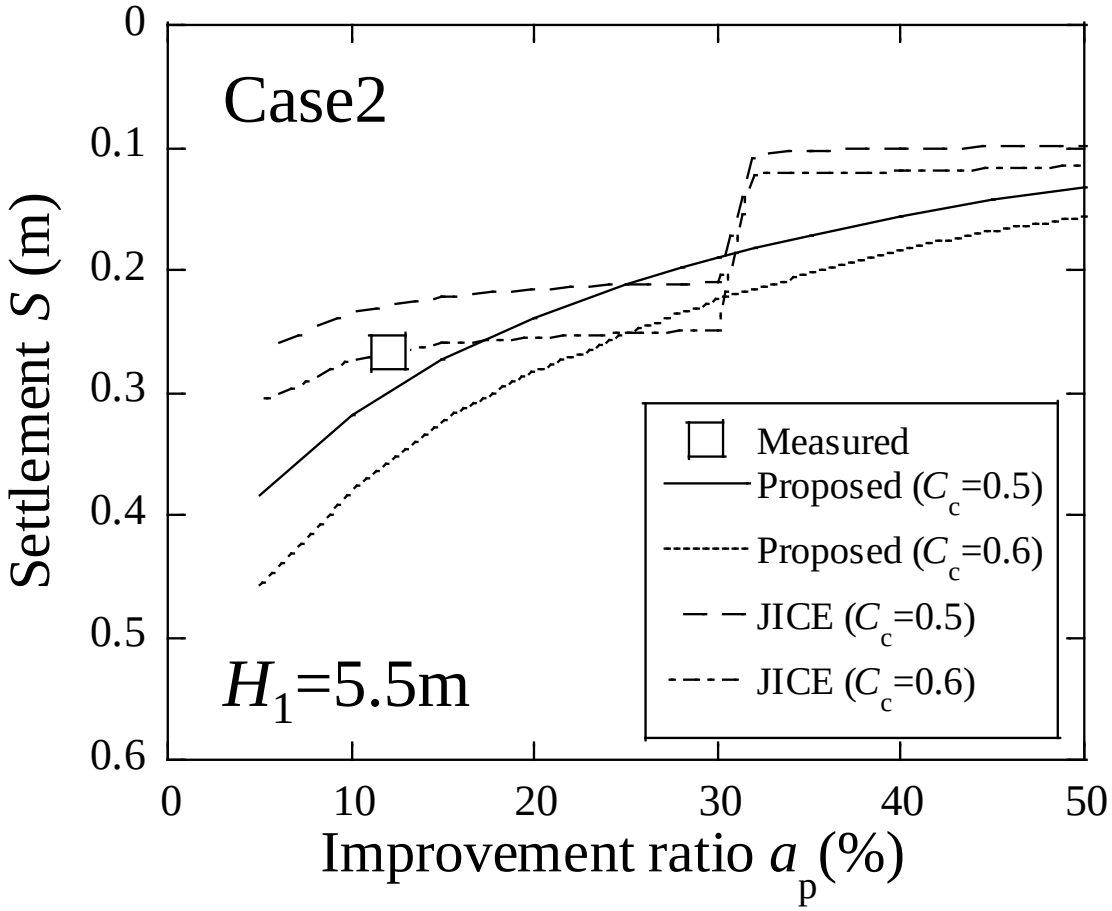

Fig.24.Comparison of calculated settlements by the proposed and JICE model with improvement ratio (Case 2).

Table1 Summary of properties for the Kaolin model clay

Properties	
Soil particle density ρ_S (g/cm^3)	2.71
Initial void ratio e_0	1.64
Plastic limit w_P (%)	31.0
Liquid limit w_L (%)	50.6
Plasticity index I_P	19.6
Compression index C_c	0.31

Table 2 Calculation process to determine the consolidating layer thickness ratio(α).

$\overline{m_v}$	Eq.(2)← $\overline{n}$: Eq.(5)← $\overline{\tau}$: Eq.(4), Degree of improvement
$\overline{m_{vf}}$	Eq.(2) ← $\overline{n} = n_f = m_v^*/m_{vs}$
m_v^*	$e - log\ p$ relationship
m_{vs}	Inverse of deformation modulus E

Table 3 Parameters determined for calculating final settlements of case studies

Confined portion		Case 1 (C_c=0.5)	Case 1 (C_c=0.6)	Case 2 (C_c=0.5)	Case 2 (C_c=0.6)
Coefficient of volume compressibility	$\overline{m_{vf}}$ (m^2/kN)	4.26E-05	4.27E-05	7.50E-04	7.57E-04
Thickness	(1-α)H_1 (m)	4.35	4.36	2.70	2.64
Average vertical stress	$\Delta\overline{\sigma}$ (kPa)	102	102	109	109

Consolidating layer		Case 1 (C_c=0.5)	Case 1 (C_c=0.6)	Case 2 (C_c=0.5)	Case 2 (C_c=0.6)
Coefficient of volume compressibility	m_v^* (m^2/kN)	8.78E-04	1.05E-03	6.67E-04	8.01E-04
Thickness of consolidating layer	H-(1-α)H_1 (m)	3.65	3.64	4.11	4.16
Average distributive vertical pressure	$\Delta\overline{\sigma}$' (kPa)	94.1	94.2	100.8	100.7